



INSTITUTO UNIVERSITÁRIO EGAS MONIZ

**MESTRADO EM TECNOLOGIAS LABORATORIAIS EM
CIÊNCIAS FORENSES**

CHEMOMETRIC PROFILE OF GUNPOWDER

Trabalho submetido por
Miguel de Lima Caliço Serol
para a obtenção do grau de Mestre em Tecnologias Laboratoriais em
Ciências Forenses

outubro de 2022



INSTITUTO UNIVERSITÁRIO EGAS MONIZ

**MESTRADO EM TECNOLOGIAS LABORATORIAIS EM
CIÊNCIAS FORENSES**

CHEMOMETRIC PROFILE OF GUNPOWDER

Trabalho submetido por
Miguel de Lima Caliço Serol
para a obtenção do grau de Mestre em Tecnologias Laboratoriais em
Ciências Forenses

Trabalho orientado por
Prof. Doutor Carlos Eduardo Proença Família

e coorientado por
**Prof. Doutor Samir Marcos Ahmad e Prof. Doutor Alexandre Luís de Matos
Botica Cortes Quintas**

outubro de 2022

*To my lovely girlfriend
Maria, to my parents,
Teresa and Miguel, to
my brother João and to
grandmother, Lucília.*

Acknowledgements

To my scientific supervisor, Prof. Doctor Carlos Família, for the support, the long hours of aid and patience with the writing of this document, articles and in the programming of the predictive models, as well for all the knowledge transmitted in several fields, not only in science, as well as in many others, which guidance was crucial for me to achieve what I achieve in the past year.

To Prof. Doctor Samir Marcos Ahmad, for all the encouragement and help during the experimental stage and writing of this document and the articles.

To Prof. Doctor Alexandre Quintas, which knowledge and expertise aid the concretisation of this project.

To all the other professors of the Degree in forensic sciences and of the Master in forensic sciences for all the knowledge transmitted over the last 5 years, with all the ideas and support regarding this step of my life, which I will carry for the rest of my life.

To my girlfriend, for all the support and love that allowed me to be where I am today, making me want to be better than I was the day before.

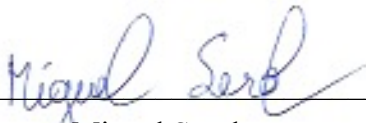
To all my family, specially to my parents, Teresa e Miguel, to my brother João and to my grandmother Lucília, to my aunts Noémia and Guida and my cousins Zé, Dulce and Alex, for all the sacrifices and struggles that went through for me to be where I am today, heart full and ready to make them all proud.

To all my friends, especially those who, like me, shared this experience and helped and support me during this work.

Declaração de Honra

Certifico que sou responsável pelo trabalho submetido neste relatório e que o trabalho é original, não sendo copiado ou plagiado de outra fonte, excetuando o especificado nas referências. Adicionalmente, declaro que o trabalho em si contido não foi submetido anteriormente para qualquer outro propósito.

Monte da Caparica, 28 de outubro de 2022


Miguel Serol

Resumo

As investigações criminais a crime onde foi utilizada arma de fogo é de extrema importância, baseando-se principalmente na análise visual de marcas em elementos munitais. Quando o invólucro ou o projétil, com essas marcas específicas da arma de fogo que disparou a munição, não estão disponíveis, é preciso encontrar abordagens alternativas para prosseguir com a investigação. Isto leva frequentemente à análise química dos compostos gerados pelo disparo da arma de fogo. Devido à pressão popular e política sobre os fabricantes, os elementos mais característicos do resíduo de disparo de uma arma de fogo, como o chumbo, antimónio e bário, estão rapidamente a ser removidos das formulações e substituídos por outros que conferem a este resíduo um menor valor probatório. Isto levou a um aumento dos estudos focados no perfil químico dos compostos orgânicos de uma munição. Estes encontram-se principalmente na carga propulsora – pólvora química. Os procedimentos mais comuns para a análise do perfil dos compostos químicos em resíduo de disparo de arma de fogo são os espectroscópicos e os cromatográficos.

Neste trabalho, propomos o uso de microextração de fase sólida em combinação com cromatografia gasosa acoplada a detetor de ionização de chama e ainda Espectroscopia de Infravermelho com Transformada de Fourier com Refletância Total Atenuada para avaliar o seu potencial discriminativo relativo à determinação do perfil químico de várias amostras de pólvora química. Nos resultados são visíveis diferenças entre amostras de diferentes fabricantes e modelos de munições. Os dados obtidos foram usados para treinar e validar modelos preditivos, com o objetivo de identificar o fabricante e o modelo de munições específicas. Os resultados obtidos apresentam uma precisão de cerca de 60% dos modelos preditivos quando classificam dados que não foram usados no seu treino. Problemas relacionados com a aquisição de dados podem ter prejudicado a precisão do modelo, sendo que overfitting dos modelos é também uma possibilidade. Contudo, estes resultados provam que esta abordagem analítica, aliada aos modelos preditivos desenvolvidos, tem um elevado poder discriminatório na identificação dos fabricantes e modelos de munições específicas.

Palavras-chave: Pólvora, GC-FID, SPME, Perfil químico; Quimiometria; Modelos preditivos.

Abstract

The forensic investigations regarding firearm-related crimes are of paramount importance, focusing mainly on visual analysis of marks in firearm-related elements. When the cartridge or the projectile, printed with specific marks from the firearm who fired the round, are not available, the analysis needs to find alternative approaches to continue with the forensic investigation. This often leads to the chemical analysis of the compounds created when the firearm is discharged. With the popular and political pressure on manufacturers, the most characteristic elements of gunshot residue, such as lead, antimony and barium, are quickly being removed from the formulations and replaced with others that grant gunshot residue chemical analysis less probatory value. This led to an increase in studies focused on the organic compound profiles of the ammunitions. These are mainly located in the propellant – smokeless gunpowder. The most common procedures for the profile analysis of chemical compounds in gunshot residues are spectroscopy and chromatography.

In the present work, we propose the use of solid-phase microextraction in combination with Gas Chromatography-Flame Ionisation Detection and Attenuated Total Reflectance-Fourier Transform Infrared Spectroscopy to evaluate their discriminative capability for the determination of chemical profile of different gunpowder samples. The results showed visible differences among samples from different manufacturers and models. The obtained data was used in for training and validation of predictive models, with the objective of identifying the manufacturer and model of specific ammunitions. The results showed an overall accuracy of around 60% when classifying data not used for the predictive model. Problems in data acquisition may have harmed the predictor's accuracy, while overfitting of the models is also a possibility. Nevertheless, these results showed that the analytical approaches and predictive model herein proposed have great potential for identifying specific ammunition manufacturers and models.

Keywords: Gunpowder; GC-FID; SPME; ATR-FTIR; Chemical profile; Chemometrics; Predictive modelling.

Table of Contents

Resumo	1
Abstract.....	3
List of Figures	7
List of Tables	9
Abbreviations.....	11
1. Introduction.....	15
1.1. Main components of intact gunpowder and gunshot residues	16
1.1.1. Inorganic compounds.....	17
1.1.2. Organic compounds	18
1.1.3. Potential sources of SG and GSR compounds	19
1.2. Analysis of gunpowder and gunshot residues.....	20
1.2.1. Morphological analysis	20
1.2.2. Chemical analysis	21
1.2.3. Sample preparation	23
1.2.3.1. Attenuated Total Reflectance (ATR).....	23
1.2.3.2. Solvent Extraction	24
1.2.3.3. Solid Phase Microextraction (SPME)	24
1.2.3.4. Headspace Sorptive Extraction (HSSE)	27
1.2.4. Spectroscopy	28
1.2.4.1. Fourier-Transform Infrared (FTIR).....	28
1.2.4.2. Raman Spectroscopy	29
1.2.5. Chromatography.....	32
1.2.5.1. Liquid Chromatography	32
1.2.5.2. Gas Chromatography.....	34
1.3. Chemometric Tools	36
1.4. Present Work	40
2. Materials and Methods.....	41

2.1.	Standards and Samples.....	41
2.2.	Gunpowder collection and preparation	42
2.3.	Spectra acquisition	42
2.4.	SPME optimisation.....	42
2.5.	SPME/GC-FID Chromatograms acquisition.....	43
2.6.	Data pre-processing and analysis.....	44
3.	<i>Results and Discussion</i>.....	45
3.1.	ATR-FTIR Spectra.....	45
3.2.	SPME optimisation.....	50
3.3.	SPME/GC-FID of intact and burnt gunpowder	52
3.4.	Training and Validation of the Predictive models	63
4.	<i>Conclusion</i>.....	67
5.	<i>Future Perspectives</i>.....	69
6.	<i>References</i>.....	71
7.	<i>Appendix</i>	

List of Figures

Figure 1 - Schematical representation of a standard "rimfire" .22 cartridge (left) and a standard "centrefire" ammunition (right).	16
Figure 2 – Example of intact gunpowder grains (adapted from Pun (70)).	21
Figure 3 – Schematic representation of headspace SPME extraction procedure.....	25
Figure 4 – Normalised ATR-FTIR spectra of the fingerprint region of the 20 analysed samples, with the 4 replicates.....	49
Figure 5 – Normalised spectra of the fingerprint region of 3 different samples (ammunition from Eley Tenex, Eley Club and Aguila Interceptor).	49
Figure 6 – SPME/GC-FID chromatogram of the analysis of the model ammunition used of optimisation experiments. This allowed the identification of the most abundant peaks (peak 1, peak 3 and peak 6). This was used to evaluate the optimisation assays	51
Figure 7 – CCD optimised response, evaluating the area of the peaks 1 (top), 3 (middle) and 6 (bottom), when different temperature and time of exposure were used.....	52
Figure 8 – SPME/GC-FID chromatograms of selected analytical standards analysed by the proposed method.	53
Figure 9 – Visual representation of the evaluation of the plots for baseline correction (Eley Force High-Velocity assay).....	55
Figure 10 – Normalised SPME/GC-FID chromatograms of intact gunpowder of the 20 analysed samples, with the 4 replicates (RT below the IS peak was removed).....	59
Figure 11 – Normalised SPME/GC-FID Chromatogram of intact SG 3 different samples (ammunition from Eley Tenex, Eley Club and Aguila Interceptor).	59
Figure 12 – Normalised SPME/GC-FID chromatograms of burnt gunpowder of the 20 analysed samples, with the 4 replicates (RT below the IS peak was removed).....	62
Figure 13 – Normalised SPME/GC-FID Chromatogram of burnt SG 3 different samples (ammunition from Eley Tenex, Eley Club and Aguila Interceptor).	62

List of Tables

Table 1 – Summary of some spectroscopic techniques employed in GSR analysis.	31
Table 2 – Summary of some LC techniques employed in GSR analysis.....	34
Table 3 – Summary of some GC techniques employed in GSR analysis	36
Table 4 – Summary of some chemometric tools employed in GSR analysis.	38
Table 5 – Manufacturer, model and country of origin for the samples used in the present study.	41
Table 6 - Experimental parameters and response values (peak area) of the CCD used to optimise the extraction of volatile compounds in smokeless gunpowder.....	50
Table 7- Retention time of selected analytical standards analysed by SPME/GC-FID..	53
Table 8- Accuracy of tested predictive models (column “Pre-Process” does not include the pre-process expressed in 3.4.1).	65

Abbreviations

2-nDPA	2-nitrodiphenylamine
2,4-DNT	2,4-Dinitrotoluene
2,6-DNT	2,6-Dinitrotoluene
4-nDPA	4-nitrodiphenylamine
AAS	Atomic Absorption Spectroscopy
AFM	Atomic Force Microscope
AK I	Akardite I
AK II	Akardite II
ANN	Artificial Neural Networks
ASTM	American Society for Testing and Materials
ATR	Attenuated Total Reflectance
CAR	Carboxene
CCD	Central Composite Design
CDR	Cartridge Discharge Residues
CMV	Capillary Microextraction of Volatiles
CSV	Coma-Separated Values
DAD	Diode Array Detector
DBP	Dibutyl Phthalate
DESI	Desorption Electrospray Ionization
DPA	Diphenylamine
DVB	Divinylbenzene
EC	Ethyl Centralite
ECD	Electron Capture Detector
EU	European Union
FDR	Firearm Discharge Residue
FID	Flame Ionization Detector
FTIR	Fourier-Transform Infrared
GC	Gas Chromatography

Chemometric Profile of Gunpowder

GSR	Gunshot Residue
HCA	Hierarchical Cluster Analysis
HPLC	High Pressure Liquid Chromatography
HS	Headspace
HSSE	Headspace Sorptive Extraction
IGSR	Inorganic Gunshot Residues
IMI	Imperial Metal Industries
IMS	Ion Mobility Spectroscopy
IR	Infrared
IS	Internal Standard
KNN	k-Nearest Neighbours
LC	Liquid Chromatography
LR	Long rifle
MARS	Multivariate Adaptive Regression Splines
MC	Methyl Centralite
MECK	Micellar electrokinetic capillary electrophoresis
MS	Mass spectroscopy
N-n-DPA	N-nitrosodiphenylamine
NAA	Neutron Activation Analysis
NC	Nitrocellulose
NG	Nitroglycerine
NIR	Near Infrared
NN-DPF	N,N-diphenylformaldehyde
NPD	Nitrogen-Phosphor Detector
NQ	Nitroguanidine
OGSR	Organic Gunshot Residues
PA	Polyacrylate
PCA	Principal Components Analysis
PDMS	Polydimethylsiloxane
PETN	Pentaerythritol Tetranite

Abbreviations

PLS-DA	Partial Least Square - Discriminant Analysis
RF	Random Forests
RT	Retention Time
SEM-EDX	Scanning Electron Microscope Coupled with Energy-Dispersive X-ray spectroscopy
SFC	Supercritical Fluid
SG	Smokeless Gunpowder
SLA-ICPMS	Scanning Laser Ablation - Inductively Coupled Plasma – Mass Spectroscopy
SPME	Solid Phase Microextraction
SVM	Support Vector Machines
TD	Thermal Desorption
TEA	Thermal Energy Analysis
TOF	Time-of-flight
UHPLC	Ultra-High Pressure Liquid Chromatography
UV	Ultraviolet

1. Introduction

Security is at the forefront of public policy, and it is one of the primary concerns of law-enforcing agencies across the globe. A widely recognised threat to safety is firearms (1,2), as their use or misuse is responsible for thousands of death every year. For example, in 2019, there were 250,000 estimated deaths related to firearms worldwide, of which approximately 177,000 resulted from physical violence, 20,000 from unintentional firearm cases, and 53,000 from self-harm. In the United States of America alone, in 2019, there were approximately 37,000 deaths associated with firearms, of which 13,000 resulted from physical violence, about 650 from unintentional firearm cases and 23,000 from self-harm. By comparison, in the European Union (EU), where the purchase of firearms is heavily regulated (3), in the same year, there were almost 6,500 deaths associated with firearms, of which around 1,000 resulted from physical violence by firearms, 380 from unintentional firearm cases, and 5,000 from self-harm by firearms (4). Also in 2019, in Portugal, one of the safest countries in the world (5), there were 211 deaths related to firearms, from which 47 resulted from physical violence by firearm, 8 from unintentional firearm cases, and 156 from self-harm by firearms (4). The sheer number of occurrences worldwide emphasises the need for a reliable framework for the forensic analysis of evidence derived from firearms use – Forensic Ballistics.

Ballistics is the discipline dedicated to study of the movement and behaviour of projectiles through the air. These study may focus on different parts of the projectile trajectory, allowing the division of this discipline into internal ballistics, external ballistics and terminal ballistics (6–9). The forensic analysis of firearms relies primarily on forensic ballistics, which comprehends the visual examination of engraved or printed marks on firearm-related elements, such as those on projectiles and casings, and subsequent comparison against samples obtained from a suspect firearm or references present in databases (6–10). Whenever this physical analysis of firearm-related elements is not possible, the chemical analysis of gunshot residues (GSR) may assist in the investigation, since it provides additional information that can also provide additional information, which can provide the basis for estimating the firing distance and time since discharge, or even the identification of the corresponding model and manufacturer of the ammunition used (6,11,12), which can ultimately lead to the identification of the suspect (12–20).

1.1. Main components of intact gunpowder and gunshot residues

The most common type of ammunition currently in use is single-use cartridges, which contain, in a single case, the primer, the propellant, and the projectile, as schematically represented in Figure 1 (9,20,21). Depending on the percussion method, ammunition is distinguished in rimfire and centrefire cartridges. The former is used primarily on .22 calibre cartridges and the latter in higher calibres (7).

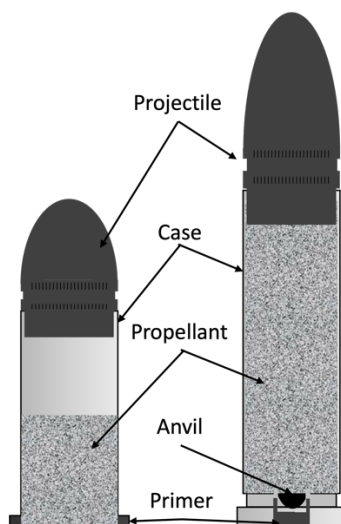


Figure 1 - Schematical representation of a standard "rimfire" .22 cartridge (left) and a standard "centrefire" ammunition (right).

The weapon's discharge occurs when the trigger is pulled, releasing the firing pin, which interacts mechanically with the base rim or centre of the cartridge and ignites the primer. This ignition deflagrates the propellant, rapidly generating a large volume of gases that thrust the projectile through its trajectory (20). This process produces the mixture known as gunshot residue (GSR). This mixture, also known as cartridge discharge residues (CDR) or firearm discharge residues (FDR) (13,21), GSR usually consists of burnt and partially burnt fragments from the primer and propellant, as well as particles from the cartridge case and the firearm itself (17,21–25). These residues escape through the firearm's openings after discharge and can deposit themselves onto any surface in its vicinity. However, some of the particles stay inside the cartridges and barrel of the gun (26–28). Due to the chemical complexity of the primers and propellants, these residues are complex and heterogeneous mixtures of compounds.

The primer currently found in most ammunition consists of a mixture of highly sensitive explosives (7) and other compounds, such as fuel, sensitisers and oxidisers (20). In modern primers, the primary explosive is lead styphnate, with barium nitrate as the primary oxidiser (7,20). The main propellant currently used in modern ammunition is smokeless gunpowder (SG), which is characterised by its high burning efficiency, high volume of gas production, low amount of smoke and debris produced with its deflagration (6,20). The primary explosive used in SG can be single-based (containing only nitrocellulose (NC)), double-based (containing NC and nitroglycerine (NG)) or triple-based explosive (containing NC, NG, and nitroguanidine (NQ)) (16,17,20,29,30). The former are the most common type of explosives in commercially available ammunition, whereas the latter is used primarily in military calibre ammunition (17,31). In addition to the primary explosive, SG can have other components, such as stabilisers, plasticisers, coolants, surface lubricants, flash inhibitors, and sensitisers (6,20,29,32–35). These compounds significantly change the chemical and physical properties of the gunpowder and allow it to perform according to the specific purpose of its design (16,32–35).

Interestingly, it is precisely the chemical complexity of propellant and primer formulations currently in use, and consequently of the GSR, that allows the discriminative analysis of GSR and SG, which assists in the investigation, in the context of forensic analysis (17,28,33).

1.1.1. Inorganic compounds

The inorganic compounds found in gunshot residues (IGSR) derive mainly from the primer, which traditionally contains antimony sulphide, barium nitrate, lead styphnate and dioxide, calcium, silicon, and tin (17,19,32,36). Due to their high molecular mass and low abundance in nature, Sb, Ba and Pb have been the main target of IGSR analysis (21,23,24,32,37,38). In fact, the ASTM 1588-17 standard (39), the Scientific Working Group on Gun Shot Residue (SWGSR) guidelines (36), and the European Network of Forensic Science Institutes (ENFSI) recommendations (40) focus on the analysis of these elements through scanning electron microscopy with energy dispersive X-ray (SEM-EDX). This is a non-destructive technique that provides robust morphological and chemical information about the sample particles (25,36,39,40). Other methods for the analysis of IGSR, not included in these recommendations, include atomic absorption

spectroscopy (AAS), atomic force microscopy (AFM), proton-induced X-ray emission (PIXE) and neutron activation analysis (NAA). AAS provides quantitative and elemental information (14,16), whereas AFM allows a very high-resolution picture of the GSR particles at the nanoscale dimensions (41). On the other hand, PIXE is a technique that employs a beam of high-energy particles for elemental analysis (42), and NAA is a highly sensitive approach that focuses on the nucleus of the atoms present in the elements of the sample with quantitative capabilities (17,43). Moreover, mass spectrometry with inductively coupled plasma (ICP-MS) also proved valuable for IGSR analysis (15,17).

GSR chemical analysis mainly targets inorganic compounds, particularly those with heavy metals, as their co-occurrence was characteristic of GSR. However, with the increase in environmental awareness (44,45) and with the USA (46) and EU (47) pushing to ban the use of lead-containing ammunition in areas such as wetlands and ponds, new primer formulations are being adopted, in which heavier elements, such as Pb, Sb, and Ba, are replaced by copper, zinc, titanium, strontium, iron, nickel, zirconium, steel and aluminium, or other more environmentally friendly organic compounds, such as tetracene, pentaerythritol tetranite (PETN), trinitrotoluene, tetryl, dextrin, diazodinitrophenol, and diazonitrophenol (16,17,19,23,44,45).

Consequently, the compounds on IGSR particles from newer ammunition are less characteristic of gunshot residues since they are naturally present in the environment, and therefore, the probative value of IGSR has diminished considerably (13,23,24). To overcome this difficulty, some researchers suggested shifting the target of GSR analyses to organic compounds or to organic and inorganic compounds combined, which recent studies suggest having higher evidential value (7,17).

1.1.2. Organic compounds

The organic compounds of SG are present mainly in gunpowder (16,24), serving as explosives, sensitisers, stabilisers, flash-inhibitors, moderants, coolants, anti-wear additives and plasticisers (17,35,48,49). The organic compounds of gunshot residue (OGSR) originate from the deflagration of the propellant. In specific cases, OGSR can also originate from the lubricants and other products used to clean firearms barrels (16,24). Currently, there are over 130 compounds associated with these residues detected and identified (16,17,48), including NC, NG, NQ, nitrobenzene (explosive), methyl

centralite (MC – stabiliser and plasticiser), ethyl centralite (EC – stabiliser and plasticiser), akardite I (AK I – stabiliser), akardite II (AK II – stabiliser) 2,4-dinitrotoluene (2,4-DNT – flash suppressor), 2,6-dinitrotoluene (2,6-DNT – flash suppressor), dibutyl phthalate (DBP – plasticiser), diphenylamine (DPA – the primary stabiliser in single-base gunpowder) and its derivatives, 2-nitrodiphenylamine (2-nDPA), 4-nitrodiphenylamine (4-nDPA) and N-nitrosodiphenylamine (N-n-DPA) (16,17,19,21,50–53).

The most common are NG, EC, MC, DPA and its derivatives (51,54), and consequently, are usually selected as target analytes due to their low abundance in the environment and uniqueness when found together, granting a high probative value (24,35,51,54–57). Interestingly, many of these additives do not go through the combustion process, which allows their detection on gunpowder and GSR samples (17,58).

Organic compounds can also originate from the primer, especially in newer ammunition models. Several patented primers use organic alternatives to lead styphnate (16,44), such as nitropentene styptic acid, tetrazene, acetogen, polinitropolyphenylether, polinitrophenylether, hexogen, polyvinyl acetate, and red phosphorus stabilised with an acid scavenger and a polymer (16,59). The analysis of these organic compounds is usually performed through infrared (IR) spectroscopy, Raman spectroscopy, as well as liquid chromatography (LC) or gas chromatography (GC), often coupled to mass spectrometry (MS) or tandem mass spectrometry (MS/MS) (19,20,23,32), described in the following sections.

1.1.3. Potential sources of SG and GSR compounds

The widespread existence of GSR-like particles in the environment imposes a serious problem in forensic investigations as they may be confused with GSR particles (25,38). These GSR-like particles can originate from fireworks (42,60,61), stud guns (38,62), some industrial tools (63), paints (38), vehicle brakes linings (64,65) or car repair and maintenance products (38). Police officers' equipment and vehicles are susceptible to contaminate suspects and evidence with GSR particles (25,66,67). Though, this contamination was shown to be negligible (67), and the officers' implementation of simple tasks such as hand washing or hand sanitising with alcoholic gels can further mitigate this risk (66).

Several compounds commonly found in IGSR, mainly those with Pb, Sb and Ba, can also be found in the environment. For example, Pb exists in soils close to major highways and roads due to its long-term use in car fuels. In addition, Pb is still used in solder for plumbing materials, glasses, paints, and battery plates (17). Sb and derivatives (oxidates) exist in some alloys used as fire retardants in cotton and polyester blends (17). Ba is present in car grease and paints (17). Nonetheless, and despite the multiple sources from which these compounds can originate, their combined presence is a good indication of GSR since there are no environmental sources for this mixture, as mentioned previously (68,69). Some compounds commonly found in OGSR can also be found in the environment. For example, DPA, the most used stabiliser, can be found on the surface of apples, outer garments, pesticides, solid rocket fuel, tires, dyes, and veterinary medicine (68,69).

However, due to the removal of the signature-elements from the primer, and subsequently from the GSR particles and because the compounds used as replacement are more common in the environment, the selection of new target analytes is a real necessity. Imposing also the adoption of different analytical methodologies suitable for the analysis of these compounds (16,17).

1.2. Analysis of gunpowder and gunshot residues

Chemical analysis has been used to identify GSR particles in suspects, cloths, objects, and surfaces. However, over the last decade, research has been focusing on the expanding the applications of the chemical analysis of GSR particles in the field of forensic sciences, such as the estimation of firing or time since discharge have also been under study (19,49,58), or the determination of chemical profiles with discriminative potential to identify manufacturers and even models of ammunition (6,16,19).

1.2.1. Morphological analysis

The evaluation of the morphologic and physical characteristics, such as the grains' shape, colour, and size, can be essential in the analysis of both SG and GSR, as it may help to identify or exclude possible manufacturers or ammunition models (26,70), but is not part of routine analysis of GSR (70). Alongside the manipulation of the chemical composition

of SG, the shape and dimension of the gunpowder grains also have an effect on the behaviour of the ammunition, mainly regarding the burning rate (70). The shape of gunpowder grains varies, with some being the shape of a disc, while other can be shaped as a sphere and even a stick (70), as visible in Figure 2. Furthermore, these characteristics also proved helpful in the determination of shooting distances for GSR particles recovered around entry holes (41).

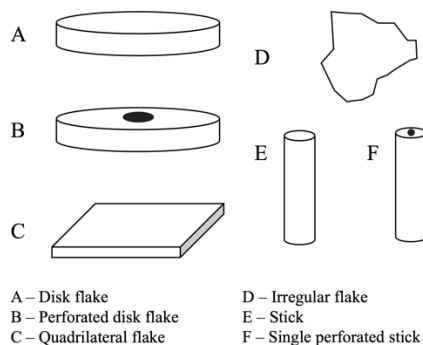


Figure 2 – Example of intact gunpowder grains (adapted from Pun (70)).

1.2.2. Chemical analysis

The first step of chemical analysis is usually the use of presumptive tests. These are simple techniques designed mainly for in-field application, and their use usually precedes more complex chemical analyses. The most common presumptive methods are colour tests, which are inexpensive, simple, and consist of rapid sets of procedures (17,20). However, since most of these tests were designed specifically for field use, they can only provide indicative results, which considerably decreases their applicability to forensic ballistics (10,16,17). In this regard, presumptive tests focus almost exclusively on identifying GSR in crime scenes, suspects or victims. Though, they can also be used to reveal the dispersion pattern found around the entry wounds of the victims and, thus, assisting in determining the firing distance (15,17).

Examples of colour tests used in forensic ballistics are the Modified Griees test (MGT), the paraffin cast or dermal nitrate tests, Walker test, Marshall and Tewari test, sodium rhodizonate test, Lunge reagent test, Harrison and Gilroy test and Zincon test. The MGT allows the determination of the total nitrite present in the GSR sample (49), while the paraffin cast or dermal nitrate test detects nitro groups, and the Walker and

Marshall/Tewari test detects nitrites. The sodium rhodizonate test detects Pb, and the Lunge reagent test detects NC. Harrison and Gilroy's test detects Pb, Ba, and Sb, while the Zincon test detects Zn and Ti, which is used in more modern lead-free ammunition (17,21,30).

As mentioned previously, the main target in the chemical analysis of ballistic elements was, for several years, the elemental analysis of IGSR through SEM-EDX, particularly heavy metals. Methods for the chemical analysis of organic compounds are still in development, and currently, there is a lack of standardised protocols or guidelines. Over the last decades, researchers began to explore the applicability of several other analytical techniques (16,18,19), optimising and exploring the limits of these approaches regarding the chemical analysis of the organic compounds of GSR or SG (34,71,72). Most of these studies focused on identifying organic compounds in OGSR through chromatographic and spectroscopic methods (73–75), the most common methodologies used in forensic chemical analysis. However, other methods were also explored, such as electrochemical analysis (76) and electrophoretic separation (56,77,78). Nonetheless, these methods successfully detected and identified only a limited number of compounds (16), hindering the establishment of guidelines and optimal procedures for this type of analysis. Furthermore, because the performance of each technique may be affected by several different variables, it may impose a case-by-case selection based on the goal of the analysis (16). The chemical analysis of OGSR should occur as fast as possible and before IGSR analysis, to minimise potential losses during storage or manipulation; due to their high volatility (24,79,80). To further prevent these losses, some authors also suggested the use of corks (81) or aluminium foil (80) to seal the end of the firearm, as well as to place the spent cartridges in hermetically sealed vials (82) between sample collection and the subsequent analysis.

To overcome the difficulties in OGSR analysis by the contamination from multiple environmental sources, several researchers suggest the addition of artificial markers in the ammunition manufacturing process (16,25). These markers would quickly help to unequivocally identify gunpowder and GSR and, possibly, manufacturers and ammunition models if each manufacturer employed different signature mixtures. Nonetheless, using these markers should not interfere with the performance of the ammunition and must be thermally stable, chemically inert, and cheap (83–86). Several ones were already suggested, including luminescent markers of the lanthanide-organic

compounds such as Europium (83,87,88), Dysprosium (89), Terbium (83,84), or other high photoluminescent metals tags (86,90). These substances were shown to maintain luminescent characteristics for up to 30 months, persist in the hands for 9 hours, and are very hard to wash off (85). However, the use of these markers may increase cross-contamination and, therefore, hinder the interpretation of the acquired data, which diminishes the evidential value of such pieces of evidence (16), rendering its usage controversial and requiring further investigations to be implemented.

1.2.3. Sample preparation

Sample preparation is essential in various analytical procedures, as it allows the extraction of the target compounds from complex matrices or the removal of interferent analytes (91) that profoundly impact these methods' analytical performance (91,92). The most common methods for SG and OGSR sample preparation are attenuated total reflectance (ATR) for spectroscopy and solvent extraction, solid-phase microextraction (SPME) and headspace sorptive extraction (HSSE) for chromatography.

1.2.3.1. Attenuated Total Reflectance (ATR)

Attenuated Total Reflectance (ATR) is one of the most used sampling techniques (93–95). ATR is a contact sampling method uses a crystal with high refractive index and good Infrared (IR) transmitting properties, which can be zinc, selenide, germanium or diamond, among others (94–96). This technique is used to measure IR spectra, based on the spectral information obtained from the reflection phenomena (95). It is non-destructive, quick and requires no sample preparation(95). It is can be used for liquid, powder or viscous samples, as well as soft materials like paper or textiles (96).

It has been used in forensic ballistics, for analysis of SG and GSR. For example, Mou *et al.* (41) developed an AFM and an ATR-FTIR procedure to discriminate between manufacturers by analysing GSR particles. Although they could not identify specific compounds in GSR samples due to the mixture of debris and other compounds, they could distinguish between manufacturers (41). Bueno and Lednev used microscopic ATR-FTIR spectroscopy imaging for the automated detection of IGSR and OGSR particles, focusing on nitrate ester compounds, specifically 2,4-DNT (97).

1.2.3.2. Solvent Extraction

Solvent extraction uses solvents with different physicochemical properties to extract selected compounds from the sample due to their different partition coefficients (98). Several solvents have been employed to extract organic compounds from intact SG (33,35,99) and spent cartridges (50), including both aqueous solutions (50,100,101) and organic solvents (30,33,35,37,99,101–105). For example, Dalby *et al.* (33) used methanol to extract selected compounds for intact SG. However, the authors noticed that most analysed samples did not dissolve completely, leading to additional centrifugation and filtration steps before GC-MS analyses (33). Dichloromethane (101,102), acetonitrile (37,99), ethanol (103), methyl-ethyl-ketone (30), and methylene chloride (35,99,104) were also used in the extraction of organic compounds of explosives, SG and GSR samples. Sauzier and co-workers (105) used acetone to extract compounds from collection devices, choosing it over dichloromethane due to its lower toxicity and ability to dissolve most explosive compounds.

Due to its inefficiency, solvent extraction has seen little use in the chemical analysis of SG or GSR, and it is now being replaced by more modern and efficient extraction methods, such as SPME or HSSE.

1.2.3.3. Solid Phase Microextraction (SPME)

Solid-phase microextraction (SPME) is a solvent-free extraction technique that allows the extraction and enrichment of volatile and semivolatile organic compounds from the vapour phase of solid, liquid and gas samples at trace or ultra-trace levels (24,33,34,71,91). The compounds in the vapour phase become adsorbed to the polymeric phase that coats the fused-silica fibre (10,16,34,91), which is usually composed of polydimethylsiloxane (PDMS), carboxene (CAR), polyacrylate (PA), divinylbenzene (DVB) or by a mixture of these sorbent phases (72,81,106–108). This extraction process results from an equilibrium established between the sample and extraction phases that is dependent on the characteristics of the sorbent coating and target compounds, the concentration of the analytes, as well as sampling temperature and time (16,33,91). After the extraction process, the analytes are desorbed from the fibre and transferred to a GC apparatus by thermal desorption in the injection port (91).

SPME, schematical represented on the Figure 3, is an environmentally friendly extraction technique because of its solvent-free nature (when thermal desorption is employed). It is also relatively cheap, sensitive and straightforward (33,91). Furthermore, it eliminates other analytical steps since the compounds can be directly transferred from the sample to the fibre and from the fibre into the injector of the GC (91,107). Despite all its advantages, SPME also has some limitations, including the inability to extract non-volatile compounds when using headspace extraction and the fact that it is mainly a laboratory-based technique, which limits its *in situ* use. Moreover, it presents low reproducibility and is more time-consuming when compared to solvent extraction (106,108). Nevertheless, this extraction technique is recurrent in several forensic areas, including explosives (109) and arson (110) investigations, as well as in forensic ballistics and gunpowder analysis (33,34,81,106–108,111).

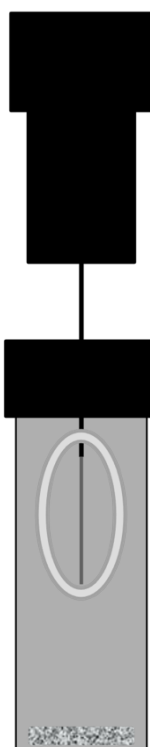


Figure 3 – Schematic representation of headspace SPME extraction procedure.

Andrasko and co-workers (81,107) were the first to employ SPME in forensic ballistics to estimate the time since discharge of several elements, namely rifles (107), pistols, revolvers (81), spent cartridges and shotguns (107). The authors focused on several OGSR using SPME combined with GC-TEA (thermal energy analysis) and GC-FID

(flame ionisation detector) (81,107). Concurrently, Chang *et al.* (71) studied three standard-loading approaches for the SPME procedure, concluding that in-vial loading of the standard is the most suitable for quantifying trace analysis of selected compounds in SG and GSR. They achieved forensic differentiation among various 9 mm calibre ammunition types by determining the volatile compounds and their relative abundance. In addition, they also found this approach suitable for detecting SG in cartridges (factory-made, homemade or illegally made) or improvised explosive devices and GSR detection (71).

In subsequent studies, Chang *et al.* evaluated SPME efficiency (111). They used 85 μm PA coated SPME fibre to extract the headspace composition of spent cartridges to detect naphthalene, DPA, 2,6-DNT, 2,4-DNT, and DBP, followed by GC-FID analyses. This approach proved successful even after repeated extractions from the same samples (up to seven times) (111). Compared with single extraction from spent cartridges, they only noted minor variations in peak areas for the selected compounds (111). Dalby and Birkett (33) also studied the effect fibre composition had on the extraction of OGSR compounds, testing seven different fibres: 65 μm PDMS/DVB, 7 μm PDMS, 30 μm PDMS, 100 μm PDMS, 85 μm CAR/PDMS, 50/30 μm DVB/CAR/PDMS, and 85 μm PA. The former was the most suitable fibre type for the analysis. In addition, they also compared solvent extraction with SPME extraction of intact SG, showing that SPME can detect the same compounds, although with GC-MS peaks with higher intensity (33).

Chang *et al.* (72) further employed a multivariate experimental design to optimise extraction-influencing parameters, including temperature and equilibrium time, to investigate the efficiency of sequential SPME in GSR of spent cartridges. They applied the extraction procedure to intact SG and successfully extracted volatile compounds that were subsequently identified by GC-FID, showing that the proposed approach can distinguish between ammunition types (72). Furthermore, Burleson *et al.* (34) developed a qualitative method to analyse single particles of partially burnt gunpowder using SPME (PDMS, 100 μm film thickness) followed by GC analysis with a nitrogen phosphorus detector (NPD), concluding that this method was suitable for analysing organic components from GSR and had possible forensic applications. They also applied their method to intact gunpowder samples, showing considerable differences in the analytical results between intact and partially burned gunpowder.

SPME was also employed in estimating time since discharge by Weyermann *et al.* (106), who developed a methodology to analyse organic volatiles residues in spent 9 mm cartridges. Optimisation of the sampling method led them to choose an 85 µm PA coated SPME fibre, with an extraction time of 40 minutes at 80°C (106). The authors identified 32 organic compounds, selecting 6 to study the potential for dating a gunshot within 32 hours after shooting. Benzonitrile, naphthalene, phenol, and 2-ethyl-1-hexanol quickly decreased 2 hours after the shot, while 1,2-dicyanobenzene and DPA decreased at a slower rate over 32 hours (106).

1.2.3.4. Headspace Sorptive Extraction (HSSE)

Headspace Sorptive Extraction (HSSE) is an extraction technique introduced recently for trace and ultra-trace analysis of volatiles and semivolatile compounds (58,112–114). HSSE has the same theoretical principles as SPME but does not use a thin fibre. Instead, it uses a magnetic stir bar coated with a much larger volume of PDMS or other phases (up to 110 µL) in comparison with SPME (up to 0.5 µL) (58). Compared to SPME, HSSE has the advantage of better extraction efficiency, higher recovery yields, and the ability to detect more compounds, which directly impact sensitivity and repeatability (10,22,58). However, to thermally desorb the extracted compounds for GC analyses, a dedicated unit must be installed in the apparatus, seriously limiting the applicability of the methodology.

Using HSSE followed by GC-MS, Gallidabino *et al.* (58) evaluated the composition and variability of volatile compounds in OGSR from nine handgun ammunition types of two calibres (.357 magnum and .45 ACP). They identified 166 compounds, mainly particles from the propellant, that did not undergo combustion (*e.g.*, additives) (58). In another study, Gallidabino *et al.* (22) evaluated the ageing of several GSR volatiles organic compounds in two types of .45 ACP ammunition using HSSE, followed by GC-MS analysis. They detected 51 GSR compounds from spent cartridges, noting significant differences in their chemical profiles, which they believed to correlate with ageing (22). They also claimed that HSSE is more reproducible and effective than SPME and allows the simultaneous analysis of more analytes (22). Compound-to-compound ratios were beneficial in reducing the variability of the ageing curve and enhancing the time window useful for production data with forensic value (22). Finally, Gallidabino *et al.* (112) also

developed, optimised, and validated an HSSE/GC-MS method to estimate the time since discharge of 9 mm cartridges, producing data which later allowed the estimation of the time since discharge through multivariate regression analysis (113).

1.2.4. Spectroscopy

Spectroscopy studies and measure the interactions between electromagnetic radiation and matter, as function of wavelength of the radiation, basing on the absorption of such radiation by vibrational states of the molecules (115). The main spectroscopic techniques used in SG and GSR analysis are Fourier-Transform Infrared (FTIR) and Raman Spectroscopy, as shown in Table 1 (14,116). IR spectroscopy relies on the interaction between infrared radiation and the functional groups in the target molecules, which will vibrate depending on the incident radiation frequency (117–120).

FTIR and Raman spectroscopy measure the interaction of energy with the molecular bonds

Since they follow different physicochemical principles and probing different vibrational modes, they can be used as complementary approaches (73,120). Raman analysis are less impacted by presence of water then FTIR and other IR techniques (115), where FTIR can be used on samples that present florescence (73).

1.2.4.1. Fourier-Transform Infrared (FTIR)

FTIR is a very versatile methodology, allowing the detection, estimation, and determination of organic compounds' chemical structure in gas, liquid or solid samples, either by absorption, emission or reflection, based on the presence or absence of specific functional groups (14,30,119–123). The chemical structure is determined based on the frequency of the absorptions bands and their relative intensity (123). For FTIR analysis, Attenuated Total Reflectance (ATR) is a common method.

For example, Brožek-Mucha (124) used IR spectroscopy combined with other techniques, such as optical and scanning electron microscopy and X-ray microanalysis, to evaluate the GSR distribution for close-range shots with a silenced gun, studying it on flesh and cloth. They showed that the silencer impacts the distribution and quantity of GSR on surfaces. Sharma and Lahiri (43) also successfully used FTIR as an alternative to

chromatographic methods to analyse OGSR, mainly to detect NG from the suspect's clothes and discussed the potential of this technique to determine the shooting distance. In another study, the same authors combined GC-MS, FTIR microscopy, and high-performance thin layer chromatography (HPTLC) and were successful in characterising and identifying explosives and explosive residues (125). Bueno and Lednev (73) reported a novel analytical and statistical methodology for the characterisation and identification of GSR. Their analytical approach focused on analysing individual particles of GSR by confocal Raman microscopy and ATR-FTIR spectroscopy, as opposed to IGSR-exclusive analysis. This approach is independent of the presence of heavy metals, which increases their usefulness for newer ammunition types (73). Subsequently, the same authors showed that ATR-FTIR has a high potential for GSR analysis and linking specific suspects with certain ammunition calibres (126).

1.2.4.2. Raman Spectroscopy

Raman spectroscopy relies on inelastic light scattering, which is correlated with the polarizability of the electrons in a molecule and provides structural fingerprints that allow molecule identification (115,120,127,128). Alongside FTIR, Raman can detect and identify IGSR and OGSR, even without heavy metals, in a fast, cost-effective, and non-destructive manner, producing IR spectra based on the radiation interaction with matter at a given wavenumber (73,121,126,129).

The first report of Raman spectroscopy applied to this field was published by López-López *et al.* (30). They were able to detect DPA and its nitration products, as well as MC, EC, and DNT. They showed that the obtained spectrums had high similarity with those of intact SG, which allowed its correlation with GSR and distinguishing between GSR-like particles (30). Subsequently, López-López and co-workers (116) used Raman with FTIR spectroscopy to compare the profiles of single, double, and triple bases SG, proving it useful as a complementary tool for rapid analysis of gunpowder compounds (116). This study showed that Raman and FTIR had discriminatory potential that depended on the sample constituents. FTIR spectroscopy showed higher discrimination capability between single-base powder with and without DNT and double-base gunpowder, while Raman showed a higher discrimination capability between gunpowder with and without DPA or DNT (116).

Apart from their studies with FTIR, Bueno and Lednev (74) also developed a methodology using Raman microspectroscopic mapping as a proof of concept to detect GSR particles. Subsequently, Abrego *et al.* (129) developed and implemented a micro-Raman spectroscopy technique to analyse OGSR and a parallel method for IGSR analysis in lead-free ammunition, using scanning laser ablation inductively coupled plasma-mass spectrometry (SLA-ICPMS). The procedure included a manual microscopical observation of GSR particles, followed by a Raman spectroscopy to detect OGSR in the samples, which allowed the identification of DPA, its derivatives, and centralites (129). Raman spectroscopy was also used by López-López *et al.* (30) and Bueno *et al.* (75) as a complement to SEM-EDX analysis (30,75). These studies showed a high correlation and identification capacity of ammunition via the obtained spectra (75). The proposed methodology is suitable for field use due to its fast, non-contact, non-destructive, solventless, and selective nature (30,75). López-López *et al.* (103) also applied surface-enhanced Raman spectroscopy to analyse SG and GSR particles after ethanol extraction. They detected several compounds, mainly EC, DPA and its derivatives.

Table 1 – Summary of some spectroscopic techniques employed in GSR analysis.

Technique	Objectives	Target Analytes	Matrix	Conclusions	Ref
Optical and scanning electron microscopy; X-ray microanalysis; Infrared spectroscopy	Evaluation of the GSR distribution for close-range shots with a silenced gun	GSR	Cotton cloth and fresh porcine skin	Attaching a silencer to the studied weapon significantly modifies the distribution and amount of GSR on the tested surfaces	(124)
ATR-FTIR and AFM	Discrimination between different manufacturers by analysing GSR particles	GSR	Polyethylene and aluminium foil sheets	Identifying specific compounds using these techniques was not possible, but different bands on FTIR spectra may help to identify the manufacturer	(41)
FTIR microscopy	Detection and estimation of NG and other GSR on suspects' hands and clothes	OGSR (mainly NG)	Cloth	A promising method to estimate the shooting distance	(43)
Raman	Identification of OGSR using Raman (first study)	MC, EC, DNT, and DPA and its nitration products,	Intact SG and GSR	Raman was a helpful screening tool for GSR, and to distinguish it from other particles; Establish a correlation between intact and burnt gunpowder	(30)
Raman and FTIR	Comparison of IR profiles obtained from both techniques. Discriminate and identify different gunpowders	OGSR	Gunpowder solutions (in methyl ethyl ketone)	Combining FTIR and Raman spectroscopy with discriminant analysis proved to be a valuable tool for the classification and the possible identification of unknown samples of gunpowder	(116)
Raman and FTIR	Development of a new analytical and statistical approach to GSR analysis	OGSR	-	Both spectroscopic techniques provide complementary information	(73)
Microscopic ATR-FTIR spectroscopy imaging	Automated detection of IGSR and OGSR particles using automatic visual scanning	GSR	Cloth (followed by tape lifting)	New automatic method to detect macro and microscopic particles and determine the "vibrational fingerprints"	(97)
Raman microspectroscopic	Chemical mapping and automated GSR particles detection	GSR	Cloth (followed by tape lifting)	Development of a procedure which is not dependent on heavier metals in GSR	(74)
ATR-FTIR	Establish a link between evidence and suspects	GSR	-	High potential for GSR analysis and linking specific suspects with certain ammunition calibres	(126)
Raman	Spectroscopically characterise and statistically explore differences in the Raman spectra of GSR of different calibre weapons	GSR	Cloth	High correlation and identification capacity of ammunition via the obtained spectra	(75)
Surface-enhanced Raman scattering (SERS)	Development of a new analytical procedure for fast and sensitive analysis of GSR	GSR	Gunpowder and GSR solutions	Detection of several compounds, mainly EC, DPA and its derivatives	(103)
Micro-Raman spectroscopy; SLA-ICPMS	Detection and identification of GSR compounds (IGSR and OGSR)	OGSR (micro-Raman); IGSR (SLA-ICPMS)	Tape-lift (modified)	Capable of detecting GSR from shooters' hands	(129)

1.2.5. Chromatography

Chromatography is a robust chemical analysis technique that enables the separation of compounds from mixtures based on their physicochemical properties. In this technique, compounds are forced to travel through a specific matrix whose characteristics lead to different interactions with each of the individual compounds found in the mixture. These interactions result in different affinities of the chemical compounds to the separation matrix, resulting in different mobilities during the chromatographic process. After the separation process, the chemical compounds go through a detector, which, similarly to the matrix, is also specifically selected based on the properties of the analytes. The signal produced by these detectors is directly proportional to the compound's concentration on the sample (130). Chromatography varies based on its stationary and mobile phases, being the most common in forensic laboratories those with a solid stationary phase and either a liquid mobile phase (liquid chromatography) or a gas mobile phase (gas chromatography) (130).

1.2.5.1. Liquid Chromatography

Liquid Chromatography (LC) is a highly sensitive and reproducible technique commonly used in forensic sciences. It is suited for separating non-volatile, semivolatile and thermolabile compounds and can be coupled with a wide range of detectors, conferring high flexibility to the technique (15). However, LC has several limitations, such as extensive sample preparation for some applications, large consumption of organic solvents, and the inability to sample gas samples, and its destructive nature (16,19). Nonetheless, several works have already explored the use of LC coupled with MS (19,37,53,54,67), diode array detector (DAD) (131,132), and ultraviolet (UV) (17,51) detectors, for forensic ballistics (Table 2).

Minzière *et al.* (32) used ultra-high performance LC (UHPLC) coupled with *tandem* mass spectrometry (MS/MS) to evaluate the simultaneous analysis of ISGR and OGSR. The authors evaluated the latter by analysing eight organic compounds commonly found in gunpowder (NG, DPA, AK II EC, 4-nDPA, 2-nDPA, 2,4-DNT, and N-n-DPA) to compare three sampling procedures. With a similar goal, Taudte *et al.* (23) used UHPLC-UV-MS/MS to develop and compare collection techniques for both OGSR and IGSR. The extraction protocol of OGSR for analysis consisted of liquid extraction with acetone

and preconcentration prior to instrumental analysis, which potentially increases the probative value of GSR when using the developed sampling method in combination with SEM-EDX and UHPLC methodologies (23). Also worth mentioning is the work of Feeney *et al.* (37), where they developed and validated an LC-MS/MS method to separate and detect both IGSR (used SEM-EDX) and OGSR in the same sample, increasing the confidence of the chemical profile. Thomas *et al.* (35) developed and employed a fast UPLC-MS/MS methodology to separate and identify analytes in GSR samples. They were successful in identifying 21 OGSR compounds. The authors were able to differentiate between brands and lots by analysing the compositional differences (35). Taudte *et al.* (51) optimised a UHPLC-UV method to separate and identify 32 OGSR compounds with lower LOD than previously reported.

In a different approach, López-López *et al.* (29) used HPLC-DAD and statistical models to predict the age of SG. They chose HPLC-DAD with an isocratic water/acetonitrile mobile phase to avoid the thermal degradation of N-nitroso-DPA when analysed by GC. The authors focused on derivatives of DPA, mainly *N*-nitroso-DPA, since the DPA nitration process is stable during the ageing of SG (29,52,133). Also focusing on the additives of gunpowder, Laza *et al.* (54) proposed an LC-MS/MS method to analyse OGSR stabilisers, such as DPA.

With a different objective, Gassner and Weyermann (53) developed a UHPLC-MS methodology to compare the efficiency of various sampling materials for collecting OGSR. The authors showed that modern instrumentation and an efficient sample preparation technique facilitated detecting and identifying OGSR from discharged material a few hours after discharge (53).

Table 2 – Summary of some LC techniques employed in GSR analysis

Technique	Objectives	Target Analytes	Matrix	Conclusions	Ref
LC-MS/MS; SEM-EDX	Separation and detection of both IGSR and OGSR in the same sample	GSR	GSR solution (in methanol and acetonitrile)	Development and validation of the methodology	(37)
UPLC/MS/MS	Separation and detection of OGSR compounds	Organic components from SG	Gunpowder solutions (in methylene chloride)	Separation and identification of 21 OGSR compounds. According to the authors, this procedure allows the differentiation between brands and lots by analysing the compositional differences	(35)
UHPLC-UV	Separation and identification of 32 target OGSR compounds, with the aid of ANN	32 OGSR target compounds	Gunpowder solutions (in dichloromethane); GSR solutions (in MTBE, after hand swab)	Separation and identification of 32 OGSR, faster and with lower LOD, thanks to ANN optimisation	(51)
HPLC	Prediction of the age of gunpowder, with the aid of statistical models	Derivates of DPA, mainly N-nitroso-DPA	Gunpowder solutions (in methanol)	Successfully determined the age of gunpowder samples using multiple linear regression with a square-root transformation model	(29)
LC-MS/MS	Development of methodologies for the analysis of OGSR to determine their application in chemical ballistic	OGSR	GSR solutions (in isopropyl/water, after hand swab)	New protocols for sample collection and preparation and analysis procedure for OGSR	(54)
UHPLC-MS	Comparison of the efficiency of various sampling materials in collecting OGSR	OGSR	GSR solutions (in methanol, after hand swab); Gunpowder solutions (in methanol)	Modern instrumentation allied with efficient sample preparation makes it easier to detect and identify OGSR from discharged material, even a few hours after discharge	(53)

1.2.5.2. Gas Chromatography

Gas Chromatography (GC) is among the most used techniques in the forensic context, in particular when coupled with mass spectrometry detector (48,92,104,134). Within the field of forensic ballistics, GC was already employed in the analysis of intact SG (33,108,135) and GSR (34,106), as presented in Table 3. This method presents many advantages, such as low analysis time, low detection limits (at the nanogram level), as well as high selectivity and sensitivity (15,17,92). However, GC is a destructive technique that can only be used to analyse volatile and semivolatile compounds, thus excluding NC and NG (15–17). Moreover, NC may decrease the GC column lifetime (17). In addition, thermally unstable compounds, such as nitrate esters (*e.g.* Pentaerythritol tetranitrate), can decompose during the analysis (16). Furthermore, this technique cannot analyse both inorganic and organic compounds, although this can be circumvented through sampling or extraction techniques that could allow separate analysis of these compounds (16).

GC has been coupled with several detectors to analyse SG and GSR, including flame ionisation detector (FID) (92,107,136), MS (24,48,92,104,134,137), ion mobility spectroscopy (IMS) (104,138), nitrogen phosphor detector (NPD) (34) and thermal energy analysis (TEA) (104,107).

GC can also be combined with thermal desorption (TD/GC), mainly when using HSSE or SPME (22). For example, Chang *et al.* (136) developed an SPME/GC-FID procedure to analyse discharged cartridges and establish the time since discharge based on the degradation of organic compounds. The quantity of these analytes was also evaluated as a function of time to estimate GSR persistence upon exposure to environmental factors (136). The results show that they successfully determined the time since discharge up to 14 days after firing, using several constituents of SG, namely naphthalene, 2,6-DNT, 2,4-DNT, DPA, and DBP. Environmental factors, such as sunlight exposure to discharged materials, were also studied (136). Weyermann *et al.* (106) also developed a SPME/GC-MS method with similar goals. This approach detected 32 OSGR in 9 mm cartridges after discharge over 32 hours. The results showed that the concentration of some compounds quickly decreased after the discharge (*e.g.*, phenol, 2-ethyl-1-hexanol, and naphthalene), while others could still be detected 32 hours after shooting (*e.g.*, DPA and 1,2-dicyanobenzene) (106).

Goudsmits *et al.* (24) developed a methodology to analyse IGSR and OGSR collected from a suspect's hands. This methodology included an SPME/GC-MS method for the analysis of OGSR and an SEM-EDX analysis of IGSR. This combined analysis allowed the authors to obtain a complete chemical profile from the GSR samples. Tarifa and Almirall (137) also combined two different rapid methodologies to characterise OGSR and IGSR to detect GSR on a suspect's hand. This approach consisted of a capillary microextraction of volatiles (CMV) followed by GC-MS and laser-induced breakdown spectroscopy (LIBS) (137).

Table 3 – Summary of some GC techniques employed in GSR analysis

Technique	Objectives	Target Analytes	Matrix	Conclusions	Ref
SPME/GC-FID	Estimate the time since discharge and environmental effects on the estimation based on the degradation of organic compounds on GSR	Naphthalene; 2,6-DNT; 2,4-DNT; DPA; DBP	Spent cartridges	Successfully detected the organic compounds in the cartridge up to 14 days after firing; Reliable determination of time since discharged based on DPA, DBP and naphthalene	(136)
SPME/GC-MS	Determination of the time since discharge of spent cartridges	OGSR	Spent cartridges	Detection of 32 OSGR in spent cartridges; DPA and 1,2-dicyanobenzenes decrease the slowest over 32 hours	(106)
SPME/GC-MS; SEM-EDX	Obtain chemical profiles of single GSR samples collected from the shooter's hands	OGSR (GC) and IGSR (SEM-EDX)	Intact SG and GSR	Successfully determined the chemical profile of samples, using the two techniques combined	(24)
SPME/GC-FID	Optimisation of an SPME procedure and determination of the viability of multiple extractions	OGSR	Spent cartridges	Spent cartridges can be analysed repeatedly and non-destructively (if appropriately sealed)	(111)
SPME/GC-MS	Determination of the most suitable SPME fibre for extracting OGSR compounds	DPA; 4-NDPA; EC; NG; DBP	Intact SG	By comparing the average peak areas of the compounds, the most suitable fibre type was determined to be the 65 µm PDMS/DVB	(33)
SPME/GC-NPD	Development of an analytical method to analyse a single particle of partially burnt gunpowder	OGSR	A single particle of partially burnt gunpowder; Intact SG	Successfully detected organic compounds in the sample	(34)
HSSE/GC-MS	Evaluate the composition and variability of volatile compounds in OGSR in handgun ammunition	OGSR	GSR (after HSSE extraction)	Identification of 166 compounds, most being additives of gunpowder	(58)
HSSE/GC-MS	Study of the ageing of several OGSR volatiles compounds	OGSR	Spent cartridges	Detection of 51 OGSR compounds, which presented noticeable ageing profiles	(22)

1.3. Chemometric Tools

The adoption of new chemical analytical techniques for detecting and identifying organic compounds in SG and GSR usually results in the acquisition of a large amount of data. Most of this data is not useful for comparison of questioned samples within forensic ballistics. However, this new abundance of data opens the possibility for the exploration of novel avenues of approach that may allow to answer to other vital questions within the field of forensic ballistics. In fact, over the last decade, several researchers have explored new applications for this data, taking advantage of the most recent statistical and machine learning tools currently available for model development (14) and of modern computational database systems for efficient storage and access to this data (139). The use of such tools applied to data resulting from chemical analysis takes the name of

chemometrics, a relatively recent field within chemistry. Within the forensic sciences, several research works have already proved the usefulness of these tools, where they helped in clustering, interpretation and optimisation of several analytical procedures, particularly those that rely on visual comparisons of spectra, chromatograms or other similar data (121,122,140–143).

Chemometric tools, which cover a wide range of applications, can be divided into three main categories: (i) pattern recognition, which can be supervised or unsupervised, and is oriented toward the automated recognition of relations in datasets; (ii) regression methods, which predict sample characteristics quantitatively; and (iii) experimental design, used to optimise chemical procedures (139).

Within forensic ballistics, pattern recognition and regression methods have already been explored to analyse SG and GSR chemical data, presented in Table 4. These methods include Hierarchical Clustering Analysis (HCA), Principal Components Analysis (PCA), Partial Least-Square (PLS), Partial Least-Square Discriminant Analysis (PLS-DA), k-Nearest Neighbour (KNN), Multivariate Adaptive Regression Splines (MARS), Random Forests (RF), Artificial Neural Networks (ANN), and Support Vector Machines (SVM) (14,51,139,144–152). HCA is a clustering method that groups objects iteratively, agglomerating or dividing clusters in each cycle based on objects' similarity for a determined distance measure (139,149). PCA is an unsupervised data reduction methodology that transforms data linearly, creating a new set of orthogonal variables that successively maximise the variance present in the data (139,148,153). PLS is a supervised regression methodology that, similarly to PCA, transforms data linearly by projecting the variables into a new space, after which a linear regression model is computed (146). PLS-DA is a supervised method that extends PLS to classification tasks (150,151). KNN is a supervised pattern recognition based on the distance between known and unknown objects, trying to group the unknown objects with their closest k-neighbours to attribute a class to the object (154). ANN are predictive models suitable for classification and regression, formed by multiple layers of interconnected perceptrons similar to biological neurons, weighing each input and producing an output (51,139,145). MARS is a non-parametric regression analysis technique that adapts linear regression methods to non-linearities interactions between variables (144,152). RF are an ensemble of independent decision trees, where each tree comprises groups of nodes representing a test on a particular object attribute (139). SVM are supervised method for classification that

separates classes based on the maximum distance between them in a hyperplane, used when known classes cannot be linearly separated (139,155).

Table 4 – Summary of some chemometric tools employed in GSR analysis.

Statistical Method	Experimental Procedure	Target Analytes	Conclusions	Ref
PCA and HCA	LC-TOF/MS	SG and OSGR	Discrimination of SG based on the chemical composition by matching SG's organic compounds to OSGR	(156)
Spearman's correlation test	HPLC and micellar electrokinetic	SG	The comparison of both techniques showed slightly different results and complementary potential	(132)
Database and analysis of the statistical impact	Raman and FTIR	GSR	Creation of a database with combined FTIR and Raman spectra; determination of the different impacts that these techniques had on a chemometric model	(73)
PLS and SVM	NIR Raman	GSR	Successful discrimination and identification of GSR particles	(75)
Likelihood Ratio	SPME/GC-MS	GSR	Creation of a logical approach to determining the time since discharge, with a successful application to a hypothetical scenario	(26)
Pairwise log-ratio normalisation combined with RF and PLS regression	HSSE/GC-MS	GSR	Estimation of time since shooting on spent cartridges	(113)
Likelihood Ratio		GSR	Evaluation of judgment and conclusions of forensic experts in Identification Ballistics, determining their results to have high sensitivity and specificity	(8)
PCA and PLS-DA	ATR-FTIR	GSR	Successful discrimination of ammunition calibre	(126)
ANN	UHPLC-UV	OGSR	Prediction of retention time of 32 OGSR compounds during method optimisation	(51)
ANN	IMS	GSR	Differentiation of particles collected by hand swabs, discriminating between shooters and non-shooters	(145)

Making use of some of these statistical analysis tools, Reese *et al.* (156) developed a non-targeted approach for characterising intact SG and OSGR. They applied their method to various ammunition from different manufacturers, calibres, and ages based on the chemical profile obtained. From this analysis, using LC/Time-of-flight (TOF)-MS, a statistical analysis was conducted using PCA and HCA to discriminate intact SG based on chemical composition and to establish a correspondence between intact SG and OSGR compounds (156).

With a different objective, Cascio *et al.* (132) used Spearman's correlation test to compare HPLC and micellar electrokinetic capillary chromatography in their capability to analyse the organic compounds of SG, obtaining slightly different results with each technique. Spearman's correlation test showed a good relationship between the different separations' patterns, pointing to the possibility of complementary approaches (132).

Bueno and Lednev (73) also reported a novel analytical and statistical methodology to analyse GSR based on the Raman and FTIR spectra dataset they compiled and pre-processed. They found that these two analytical techniques contributed differently to the chemometric model. However, they also showed this to be a robust approach in forensic investigations to rule out particular firearm ammunition (73). The same authors (75) also studied the potential of Near Infrared (NIR) Raman to discriminate and identify particles of GSR using PLS correlation analysis and SVM.

Gallidabino *et al.* (113) used chemometrics to estimate the time since shooting from spent cartridges based on their previously optimised and validated HSSE/GC-MS methodology. They tested PLS, MARS, ANN, RF, KNN and SVM regression algorithms and found the most suitable models to be those trained with RF and PLS (113).

Bueno *et al.* (126) combined ATR-FTIR with statistical analysis, PCA and PLS-DA. The PCA analysis revealed that samples from the same calibre were grouped. At the same time, the PLS-DA allowed the differentiation between the three calibres (firearm-ammunition combination) data from the three calibres analysed in the study.

Taudte *et al.* (51) applied ANN under a predictive data-processing program to predict the retention time (RT) of 32 OGSR compounds analysed by UHPLC-UV using several gradients, allowing the detection of all of the studied compounds. Bell and Seitzinger (145) have also used ANN to differentiate samples from shooters and non-shooters based on ion mobility spectra obtained from hand swabs.

In this field, the higher the sample dataset and its variety, the more effective and accurate the classifier is, but generating data in such amount, via experimental procedure is very time and resource consuming (157,158). Thus, data augmentation, a term that englobes all methods that introduce unobserved data to build a more accurate and robust classification models (157,158), is a useful tool for scientists in several areas. One possible approach is the addition of Gaussian noise to experimental data, which has been

previously used by Conlin *et al.* (159) in NIR spectroscopic data, achieving better accuracy and robustness with the adding of these synthetic data.

Regarding the visual comparison of firearm-related elements, Mattijssen *et al.* (8) used computer-based methods to evaluate the validity and reliability of judgments and conclusions of forensic experts in Identification ballistics. The procedure is based on data acquisition in 2D and 3D, followed by data-pre-processing and comparing striation patterns to calculate the Likelihood Ratio (8). The study showed the high sensitivity and specificity of the conclusions presented by the examiners. Still, they seem slightly less proficient at relating samples from the same source and better at distinguishing samples from a different source when compared with the computer-based method (8).

1.4. Present Work

Wrobel *et al.* (160) developed a tool to identify .22 calibre ammunition from GSR and other materials related to the cartridge, focusing on the heavier metals present in the primer. Their work also focused on physical characteristics and the primer chemical profiles, but in a superficial way, setting a data base with their findings. Bueno *et al.* (126) also developed a method with a similar goal, which was able to evaluate the discriminative potential of FTIR spectra of SG, focusing not on determining the manufacturer or the model, but the calibre of the ammunition.

In this work, chemical data from the propellant obtained was used in the training and validation of predictive models, with the objective of identifying the manufacturer and model of the ammunition analysed. This approach has been explored by other authors, but their focus has been on estimating time since discharge (113), age of intact SG (29), automated detection of GSR particles (97), and other applications, mentioned in 1.3.

This work aims to develop predictive models to enable the identification of the model and manufacturer of .22 Long Rifle (LR) calibre ammunitions. This ammunition calibre was selected since it is one of the most commercially successful ammunition in the world, being available in most countries. The model will be developed using chemometric tools from data experimentally determined by ATR-FTIR and SPME/GC-FID for burnt and intact SG.

2. Materials and Methods

2.1. Standards and Samples

Analytical standards of DPA (ACS, Alfa Aesar, Switzerland), 4-nDPA (> 98%, Alfa Aesar, UK), 2,6-DNT (97%, Alfa Aesar, Germany), 2,4-DNT (97%, Sigma-Aldrich, Germany), N,N-diphenylformaldehyde (99%, NN-DPF – Sigma-Aldrich, Germany), N-n-DPA (>97%, Sigma-Aldrich, Belgium), 1,3-diethyl-1,3-diphenylurea, also known as EC (98%, Sigma-Aldrich, USA) and naphthalene (99%, Acros Organic, Czech Republic) were acquired.

Ethyl benzoate (>99%), which was the selected internal standard (IS) for the chromatographic analysis was purchased from Acros Organics (Mexico). Methanol (>99,8%) used for IS solutions was purchased from Fischer Scientific (UK).

Twenty different models of .22 LR calibre ammunition were obtained in a local gun shop from Almada, Portugal. These (Table 5) included 8 different brands: Aguila (3 models); CCI (1 model); Eley (7 models); Federal Ammunition (2 models); Fiocchi (3 models); GECO (2 models); Imperial Metal Industries (IMI – 1 model – vintage); RWS (1 model).

Table 5 – Manufacturer, model and country of origin for the samples used in the present study.

Manufacturer	Model	Origin	Manufacturer	Model	Origin
Aguila	Interceptor	Mexico	Eley	Match Pistol	England
Aguila	SuperExtra	Mexico	Federal A.	American Eagle	USA
Aguila	Rifle Match	Mexico	Federal A.	Game Shok	USA
CCI	Quiet	USA	Fiocchi	F320	Italy
Eley	Force High-Velocity	England	Fiocchi	Ultra-sonic	Italy
Eley	Tenex	England	Fiocchi	TTSOFT	Italy
Eley	Tenex Pistol	England	GECO	Semiauto	Germany
Eley	Club	England	GECO	Rifle LNR	Germany
Eley	Rifle Club	England	Imperial Metal Industries	-	England
Eley	Pistol Match	England	RWS	Special Match	Germany

2.2. Gunpowder collection and preparation

Gunpowder was collected directly from the cartridges, following the removal of the projectile with the use of a vice and pliers. The cartridge's contents (intact smokeless gunpowder) were emptied into 4 mL amber glass vials (Agilent, USA), and 100 μ L of IS solution (0.105 mg/mL of ethyl benzoate in methanol) was added. For the collection and preparation of burnt gunpowder, the cartridge's contents were placed on a glass microscope slide, being burnt using a micro torch butane flame gun (Jet Torch, China). Then, it was scraped from the slide using a scalpel and moved to the inside of a 4 mL amber glass vial using a spatula. Afterwards, 10 μ L of IS solution (1.05 mg/mL of ethyl benzoate in methanol) was added. The vials were covered with a screwcap with polytetrafluoroethylene (PTFE) septum (Agilent, USA) followed by the SPME procedure.

2.3. Spectra acquisition

FTIR spectra were measured in a Perkin Elmer (EUA) Spectrum 65 FT-IR Spectrometer, with a diamond crystal (SPECAC, piece GS10801-B, UK), coupled with an ATR Specac Quest (UK). The FTIR spectra were recorded as both transmittance and absorbance values, using the PerkinElmer Spectrum software (version 10.4.1.262). Background air spectrum was collected before all sample analysis and the ATR crystal was cleaned with ethanol (96%) between all analysis. The analytical window was from 4000-550 cm^{-1} , with a resolution of 4 cm^{-1} and 9 accumulations. It was determined that the spectral region of 1800–550 cm^{-1} provided the most informative FTIR, by an evaluation of the spectra obtained, since this is the region with most bands and less noise.

2.4. SPME optimisation

The SPME procedure was optimised using a Central Composite Design (CCD), based on a 3^2 factorial design (with $\alpha = 1.414$), with 5 centre points. The parameters evaluated and optimised were exposure time and temperature. Thirteen experiments were designed by CCD, using the Minitab software (UK), version 17.1.0, and executed in a randomised order, using a sample from the study. The tested temperatures and exposure times were between 60°C and 100°C, and 20 and 60 minutes, respectively. These values were selected

based on the literature. Comparison of areas of the three peaks with the highest intensity served to monitored response variables.

2.5.SPME/GC-FID Chromatograms acquisition

Two manual SPME holders and fibres coated with divinylbenzene, carboxene and polydimethylsiloxane (DVB/CAR/PDMS, 50 µm film thickness) were purchased from Supelco (USA). The full content of the cartridge, intact or burnt, were heated in a dry bath (Bioblock Scientific, USA) at 84°C for 40 minutes, with the fibre exposed into the headspace of the vial. Afterwards, the SPME apparatus was immediately introduced to the injection port of the GC. Extracts were thermally desorbed from the fibre in the GC injection port for 5 minutes.

For the analysis of analytical standards, the exposure time was reduced to 5 minutes, the fibre was kept for 10 minutes in the injection block using a split ratio of 20:1.

Each day, the fibres were conditioned on the injector port of the GC-FID for 30 minutes, at 270°C, as manufacture's indications. Between each analysis cycle (two analysis, one on each fibre), the fibres were conditioned in the injection port of the GC-FID for 10 minutes, with the injection port at 270°C, and the oven at 280°C.

The GC analysis was performed in a 7280A chromatograph (Agilent, Germany) equipped with a split/splitless injector and a FID (Agilent, Germany). The column was a HP5-MS (5% phenyl-methylpolysiloxane stationary phase with 30 m x 0.25 mm i.d., 0.25 µm film thickness, Agilent Technologies Inc., USA) and the carrier gas was helium (Gasin, Portugal – 99,9992%), with a flow of 3 mL/min. Auxiliary air (Gasin, Portugal – 99.995%) and hydrogen (Gasin, Portugal – 99.999%) were used as detector gases at flows of 300 and 30 mL/min, respectively.

Chromatographic separations of the samples were carried out right after the SPME procedure, in accordance to similar works (34). The SPME fibre was inserted in the injection port for 5 minutes under the split mode (2:1). The initial temperature was held at 40°C for 5 min, then the temperature was ramped at 20°C/minutes for 12 minutes to a final temperature of 280°C held for 5 min. Injector and detector temperatures were set at 250° and 280°C, respectively.

2.6. Data pre-processing and analysis

The ATR-FTIR spectra used in the predictor development, were obtained using the PerkinElmer Spectrum software (version 10.4.1.262). The chromatographic data used for the predictor development was obtained using Agilent's OpenLab software, version Rev.C.01.03 [37], from Agilent Technologies (Germany). Both data types were exported as comma-separated values (CSV) files, using the respective software.

Statistical analysis was performed on the exported CSV files, using programming language R (version 4.0.4 GUI 1.74) and the program RStudio® (version 2022.07.1 RStudio, PBC). The pre-processing of the chromatographic data included data alignment, reduction of the resolution of the chromatograms, baseline correction, done resorting to the R packages 'Baseline' (161), and normalisation. The pre-processing of the spectra included only the normalisation of the spectra by maximum and minimum. For the creation of the chromatograms and spectra presented in this work, the R package 'ggplot2' (162) was employed. For the development, training and validation of predictors, the R package 'caret' (163) was used with the classification algorithms RF (164) and C50 (165).

3. Results and Discussion

3.1. ATR-FTIR Spectra

The spectra for each sample were obtained from replicates from the same model, which consisted of intact SG extracted from four different ammunitions from the same box, producing the spectra visible in Figure 4. The main objective was not to determine the composition of the samples, which, due to the nature of gunpowder and of FTIR itself, identification of individual compounds was not possible. Nevertheless, it was possible to identify some bands associated with SG, such as those corresponding to NC. NC is the main compound of single base SG (the one used on .22 LR calibre ammunition). For this reason, specific bands that correspond to functional groups nitro (-NO₂) and nitrate (-NO₃) are expected to be found in the spectra of all the samples (41,166,167). Bands matching the nitro group are visible in all the samples, with the wavenumbers of 1630 cm⁻¹ (-NO₂ asymmetric stretch), 1270 cm⁻¹ (-NO₂ symmetric stretch) and 820 cm⁻¹ (-NO stretching) (126,166–168).

All ATR-FTIR spectra were pre-processed prior to analysis. The data was trimmed, being only used the data with wavenumber between 1800 and 550 cm⁻¹, since this was the region with the most bands and less noise, evaluated by a visual analysis. The data was then normalised, which was achieved by subtracting the minimum value of the transmittance value of all the other values of transmittance of the sample and divided the result by the difference between the maximum and minimum transmittance values for each spectrum, and then multiplying the results by 100, as expressed in the following equation:

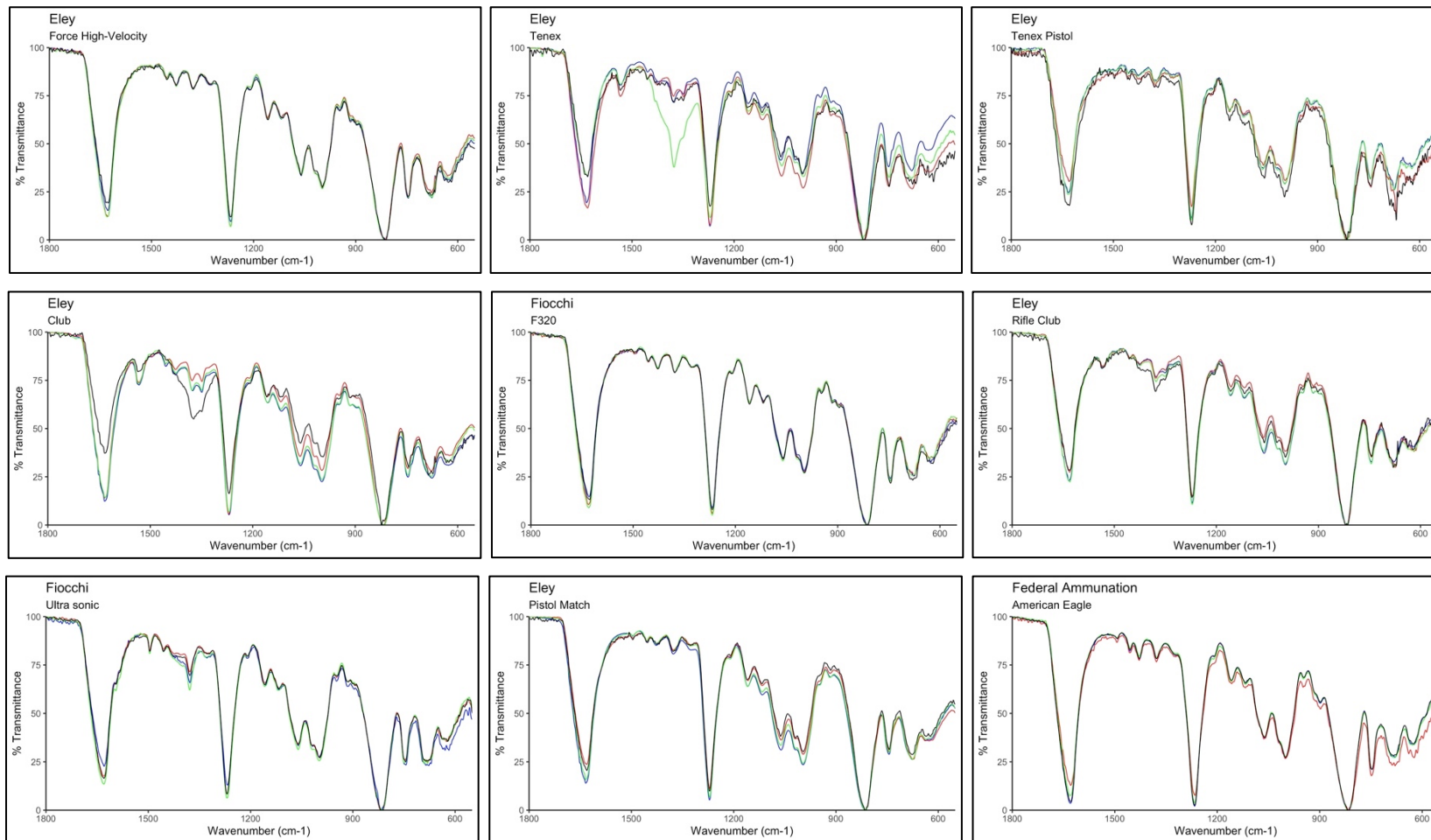
$$\text{Normalisation} = \frac{\text{Transmittance}(\text{sample}) - \text{Transmittance}(\text{min})}{\text{Transmittance}(\text{max}) - \text{Transmittance}(\text{min})} * 100$$

Where *Transmittance(sample)* is the transmittance of any point on any replicate of a sample, *Transmittance(min)* the lowest value of transmittance of the replicate of a sample and *Transmittance(max)* the highest value of transmittance of the replicate of a sample. The fingerprint region was the focus of the statistical analysis due to the absence of bands and presence of noise in the remaining spectra.

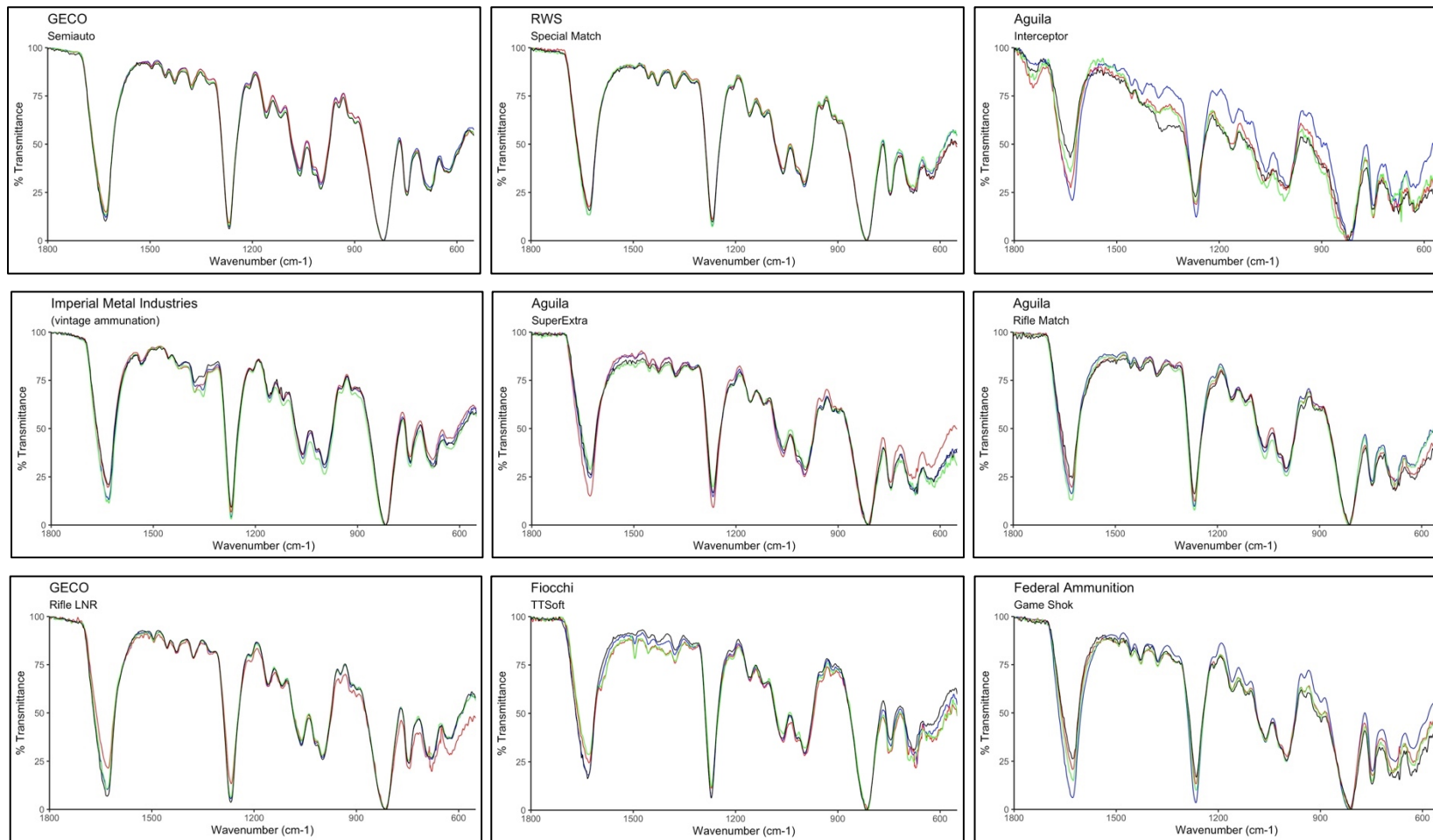
The objective of the ATR-FTIR analysis was to obtain chemical profiles of the samples, in order to determine their discriminatory potential and viability of data for a predictor. The obtained spectra showed a high similarity between the replicate analysis within sample ammunition, as can be seen in the examples in Figure 4, with some samples, after normalisation, overlapping almost completely, like Fiocchi F320 and Federal Ammunition American Eagle. On the other hand, slight differences are present in the chemical profile of samples from different manufactures and models, being mostly visible in the fingerprint region of the spectrum, as shown in Figure 5. This aligned with the previous work of Mou *et al.* (41) whom were able to distinguish between manufactures by the chemical profile of GSR samples analysed with ATR-FTIR, but were unable to identify any specific compound in any of the samples.

These differences were explored for training different predictive models in order to test the discriminative potential of chemical profiles of the analysed samples.

Results and Discussion



Chemometric Profile of Gunpowder



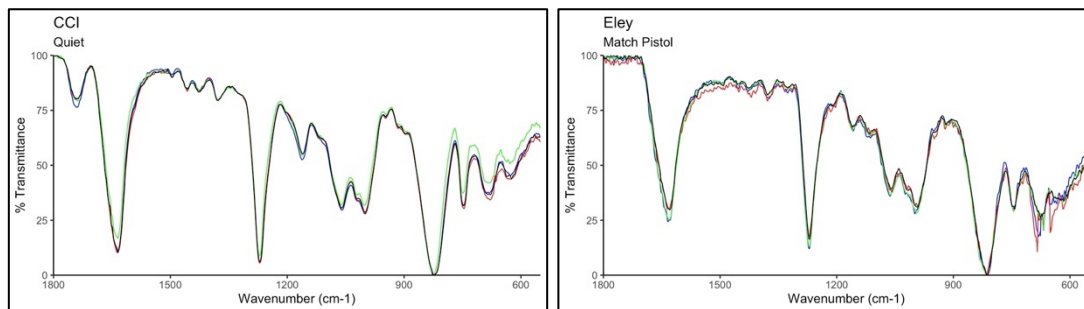


Figure 4 – Normalised ATR-FTIR spectra of the fingerprint region of the 20 analysed samples, with the 4 replicates.

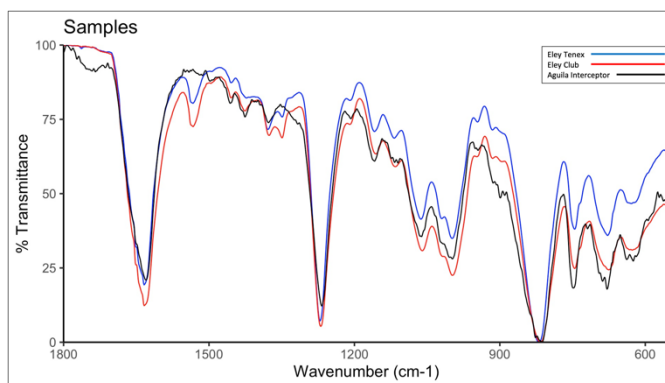


Figure 5 – Normalised spectra of the fingerprint region of 3 different samples (ammunition from Eley Tenex, Eley Club and Aguila Interceptor).

3.2. SPME optimisation

In the majority of published studies, SPME variables are optimised using an one variable at a time strategy (169), not allowing to check for factor interactions (170). For this reason, CCD was used, since it is an effective tool of optimisation, when several parameters need to be tested (169). A total of thirteen optimisation assays were performed, using samples from IMI ammunition. The assays for optimisation of the SPME procedure were conducted to find the optimal conditions for fibre exposure time and temperature needed to extract the target compounds. The areas of the three most abundant peaks were selected as criteria to evaluate the optimisation procedure. The lowest temperature assayed was 52°C, with the highest being 108°C; the longest exposure of the fibre during the optimisation tests was 68 minutes, and the lowest exposure time was only 12 minutes, as observed in Table 6.

Table 6 - Experimental parameters and response values (peak area) of the CCD used to optimise the extraction of volatile compounds in smokeless gunpowder.

Run	Extraction Temperature (°C)	Extraction time (min)	Response Value (peak area)		
			Peak 1	Peak 3	Peak 6
1	80	80	4891.9	8703.9	1731
2	60	60	3643	5206.4	164.3
3	51.7	51.7	1650.2	1577.4	105.9
4	100	60	4027.2	11190.6	6960.3
5	80	40	4466.6	13273.9	2940.5
6	80	40	5442.5	10010.4	1739.8
7	60	20	1388.8	1421.9	65.6
8	80	40	6178	8257.9	1333.1
9	100	20	5237.6	1190.8	7135.6
10	80	12	7408.1	5661.2	846.3
11	80	40	6629.9	9957.9	2458.6
12	80	40	4112.8	9951.5	2511.7
13	108.3	40	8362.3	14161.1	12736.9

All optimisation assays are expressed in Figure 6, were the 12 peaks with most intensity in the samples were presumptively selected to optimise the procedure, but only peak 1, peak 3 and peak 6 were used in the final optimisation procedure.

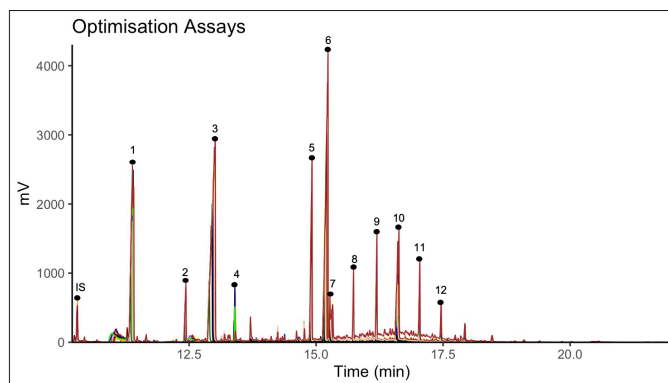


Figure 6 – SPME/GC-FID chromatogram of the analysis of the model ammunition used of optimisation experiments. This allowed the identification of the most abundant peaks (peak 1, peak 3 and peak 6). This was used to evaluate the optimisation assays .

Variation analysis (ANOVA) was applied to estimate the statistical importance of the proposed method. A p value lower than 0.05 in ANOVA indicates the statistical importance of an effect, with a confidence level of 95%. The adjustment of the polynomial model equation was expressed by the determination coefficient R^2 (61.94%) for peak 1. These values indicate that the proposed model is able to explain 61.94% of the response variability of the proposed model. The Lack-of-Fit (LOF) test, that shows the variation around the proposed model, presented a p value of 0.105, which indicates a good adjustment of the model to the responses obtained. The relation between the response and the factors is expressed by the following equation:

$$Area_{Peak1} = -19127 + 445 Temp + 179 Time - 1.70 Temp * Temp - 0.27 Time * Time - 2.17 Temp * Time$$

In the presented equation, $TEMP$ corresponds to the extraction temperature and $TIME$ the extraction time. These results show that the optimised response was obtained using a temperature superior to 84°C and an exposure longer than 40 minutes had no significant

impact in the extraction efficiency (Figure 7). The results are similar to other applications using SPME for the extraction of target compounds in gunpowder or GSR (22,24,34).

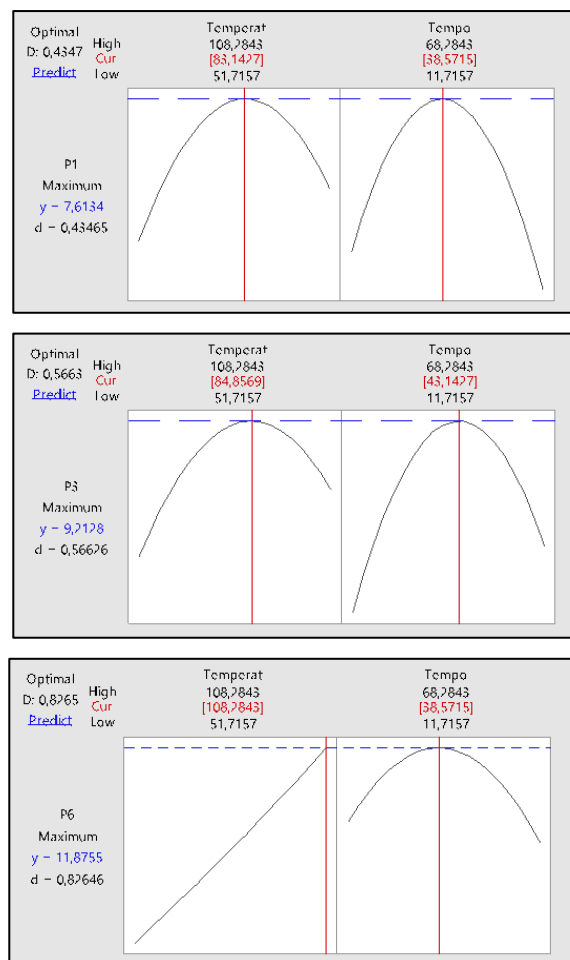


Figure 7 – CCD optimised response, evaluating the area of the peaks 1 (top), 3 (middle) and 6 (bottom), when different temperature and time of exposure were used.

3.3. SPME/GC-FID of intact and burnt gunpowder

Headspace (HS) SPME analysis of the volatile and semivolatile compounds of SG in the vial were heated in a dry bath, while the fibre was exposed to the HS of the vial, similar to Figure 3. The SPME fibre (50 µm DVB/CAR/PDMS) employed in this work was one already successfully used by Dalby and Birkett (33) to extract organic volatile and semi-volatile compounds from SG.

Like in the ATR-FTIR analysis, this analytical strategy's objective was not to determine the composition of the gunpowder formulations, but to establish their chemical profiles.

Nevertheless, and based on commonly used compounds for ammunition manufacture (17), some of the main markers of SG and GSR were selected and tested using the developed procedure to identify some of the substances detected. Solid standards of DPA, 2,6-DNT, 4-nDPA, 2,4-DNT, NN-DPF, N-n-DPA, and EC were analysed by SPME/GC-FID. The SPME/GC-FID analysis of standards produced the results in Table 7 and Figure 8. With the developed method, 4-NDPA was not detected.

Table 7- Retention time of selected analytical standards analysed by SPME/GC-FID.

Standard	Abbreviation	Role	Retention Time (min)
2,6-dinitrotoluene	2,6-DNT	Flash suppressant	12,486
2,4-dinitrotoluene	2,4-DNT	Flash suppressant and plasticiser	12,948
N-nitrosodiphenylamine	N-n-DPA	(Derivate from DPA)	13,401
Diphenylamine	DPA	Stabilizer	13,447
N, N-diphenylformaldehyde	NN-DPF	(Derivate from DPA)	14,348
1,3-diethyl-1,3-diphenylurea	EC	Stabilizer and plasticiser	14,927
4-nitrodiphenylamine	4-NDPA	(Derivate from DPA)	-

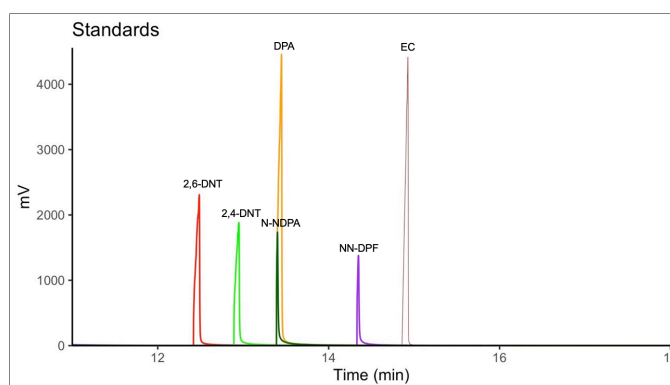


Figure 8 – SPME/GC-FID chromatograms of selected analytical standards analysed by the proposed method.

The chromatographic analysis was performed with a qualitative and semi-quantitative objective, where the presence of peaks and their average intensity were used to establish

the chemical profile of the analysed samples, which were later used to develop the predictors.

Before the development of the predictor, the data was pre-processed. The first step of the chromatographic data pre-processing was trimming, where only the data with RTs higher than that of the IS (approximately 10.3 minutes for all samples) was kept, as no peaks, except for methanol (solvent of the IS solution), were detected prior to this RT (roughly 1.5 minutes). After trimming, chromatograms were aligned using the RT of the IS as initial time ($RT_{IS} = 0$), so that the initial time would be that of the IS. Chromatograms were further stretched or compressed in the time axis because there were small deviations between identical peaks in different chromatograms, which increased with the RT. This was performed, using the RT of matching peaks (identified visually on the chromatogram plots) between a reference assay (the first replicate of Eley Force High-Velocity) and that of the sample being aligned, from which a correcting factor was determined (time of the peak in the reference sample chromatogram divided by the time of the corresponding peak in the chromatogram), as shown in the following equations:

$$Stretch = T(ref) / T(sample)$$

$$Aligned\ Time = Time(samples) * Stretch$$

Where T is the time that corresponds to the RT of the peak in the reference sample and on the sample and $Time$ corresponds to all RTs values of time in the sample.

The original resolution of the chromatograms was 50 Hz, which translates to 3,000 data measures per minutes, comprising a total of 30,000 points for the interval of the 10 minutes later considered for the analysis. Because this high dimensionality of the data could hinder the predictor training, reduction of the resolution to 200 measurements per minute was performed, which converted the original 50 Hz to around 3 Hz and led to a total of 2,000 values for the same 10 minutes interval.

After these alignment steps, all chromatograms were trimmed again so that the RT_{IS} was zero and the ending time was 10 minutes after the RT_{IS} . Subsequently, the baseline of each chromatogram was corrected, using polynomial regression from the R package 'Baseline' (161), with varied degrees of freedom, which were chosen based on a visual

evaluation of the chromatogram, given by the package, and visible in Figure 9. Lastly, the chromatograms were normalised by the intensity of the IS, according to the following equation:

$$\text{Normalisation} = \frac{I(\text{sample})}{I(\text{IS})} * 100$$

Where $I(\text{IS})$ is the intensity of the peak that corresponds to the RT_{IS} , and $I(\text{sample})$ is the intensity of the remaining peaks on the chromatogram.

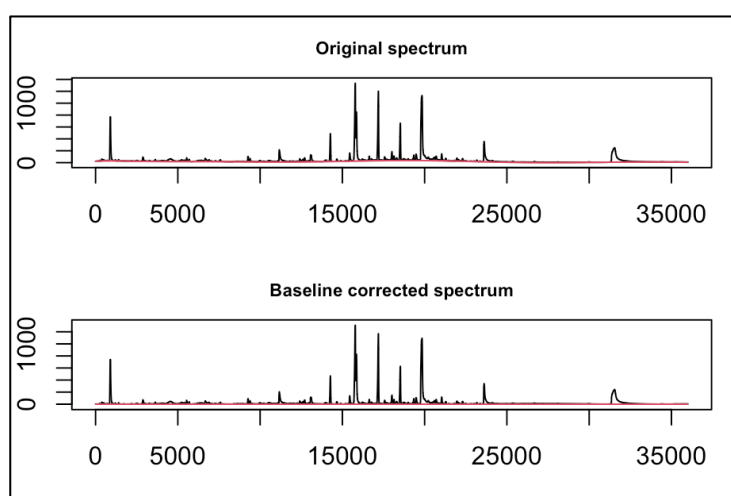


Figure 9 – Visual representation of the evaluation of the plots for baseline correction (Eley Force High-Velocity assay).

Regarding intact SG samples (Figure 10), not every analysed sample produced a very rich chromatogram. This may be related with the grain coating of the specific gunpowder, which could have prevented the volatilisation of the organic compounds, a problem that an extra sample preparation step, such as fine grinding the gunpowder grains, may help overcome.

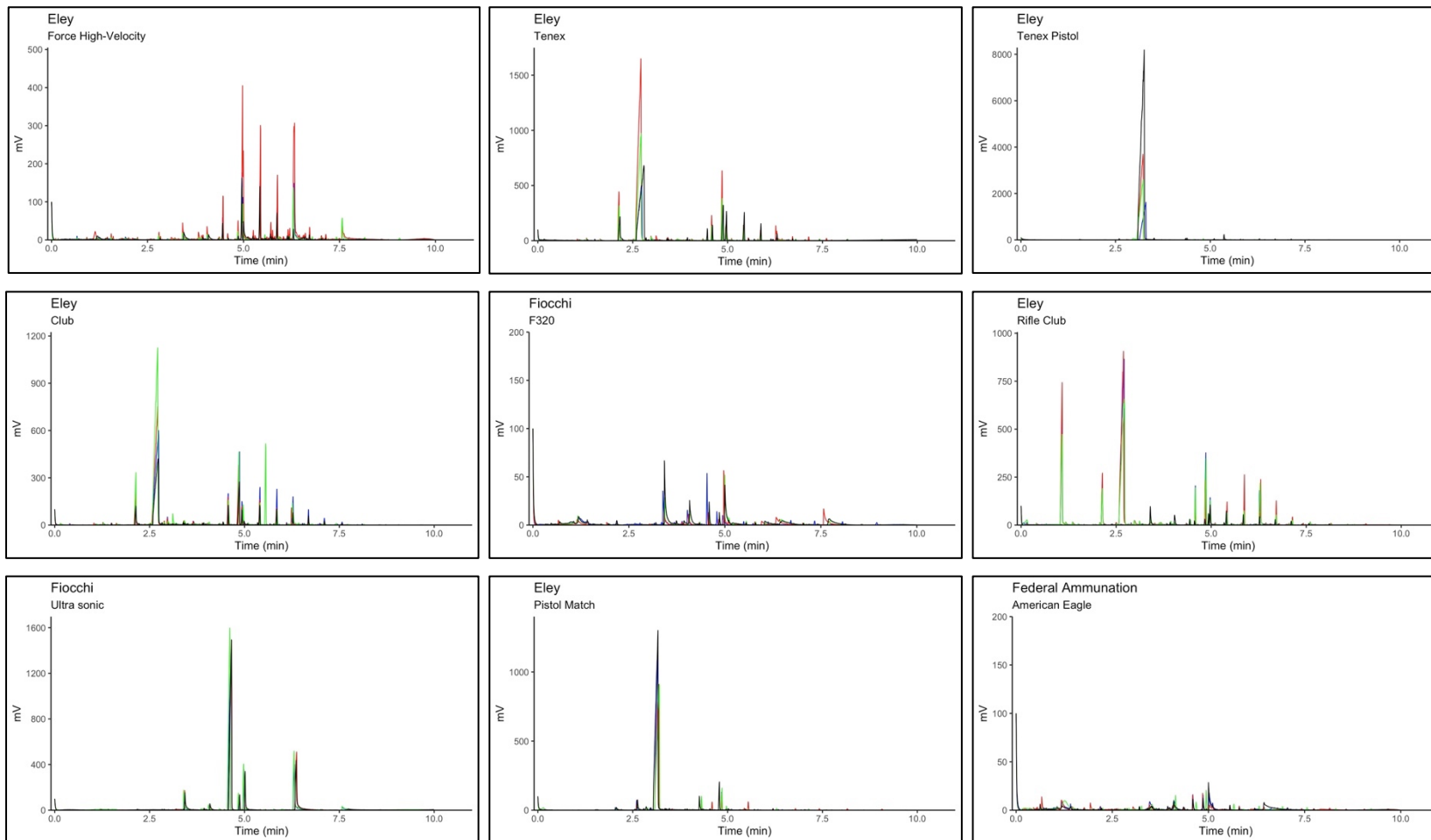
The results show that distinct chemical profile of each SG sample was obtained, similar to the results of Thomas *et al.* (35). These authors were able to differentiate between brands and lots by analysing the compositional differences, using UPLC-MS/MS. For example, as shown in Figure 10, peak overlapping in the replicates belonging to the same sample is clearly visible. On the other hand, when different samples are used, distinct chemical profiles were obtained, as visible in Figure 11. This shows the potential for

discriminatory capability of the proposed analytical approach. In order to use this potential, a more complex computing and statistical analysis is required. Chemometric data can be used with statistical analysis tools to produce a predictive model.

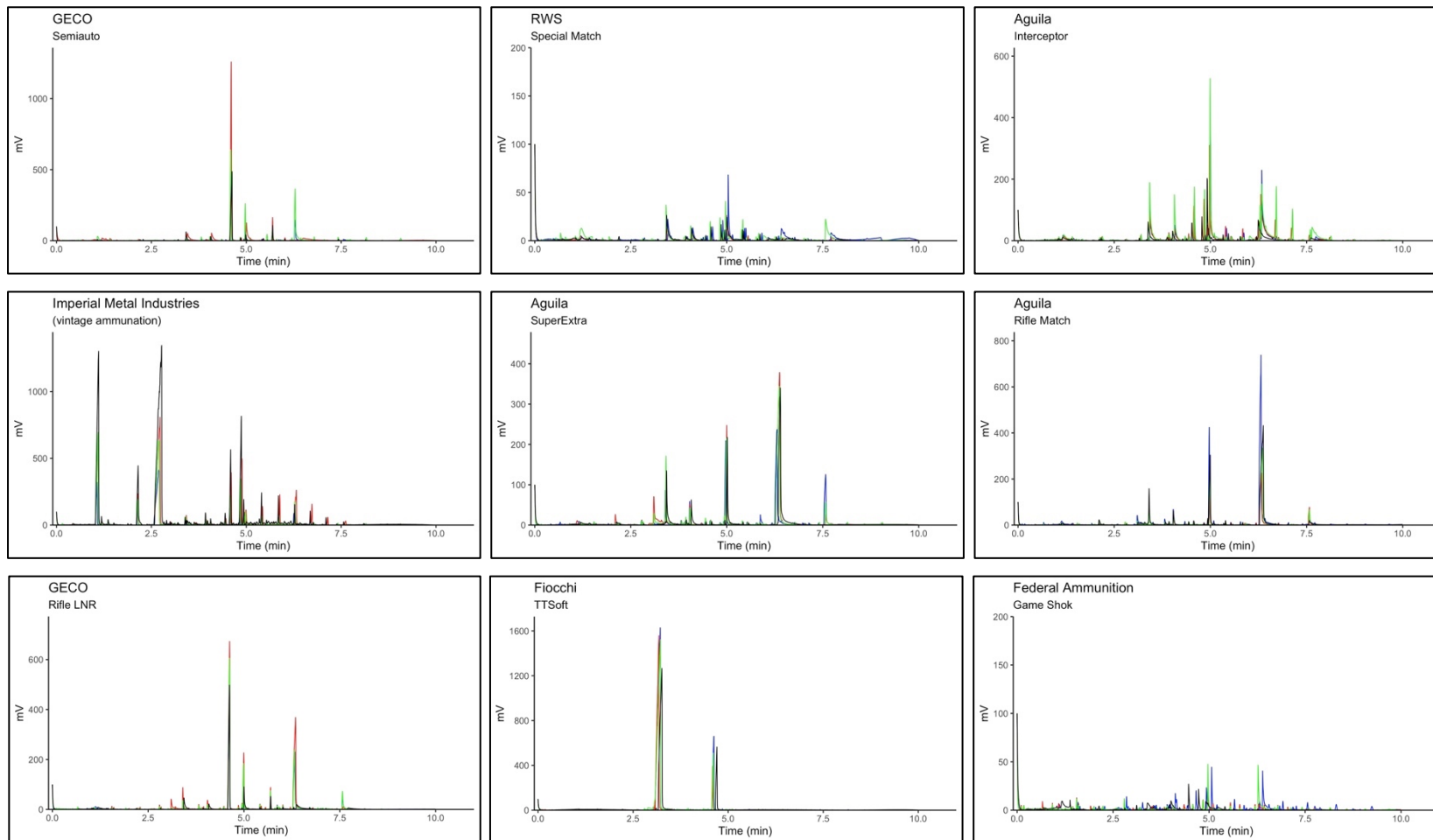
Burnt SG samples were analysed by SPME/GC-FID. The produced chromatograms (Figure 12) present more differences amidst replicates of the same sample, since the procedure used to obtain the burnt SG may allow the analysis of intact SG grains mixed in the burnt mixture, so the results are less reliable. Nevertheless, this data was also used in the development of a predictor, since differences were visible among samples different of different manufacturers and models (Figure 13). The models trained with these data were not expected to achieve great success due to the variability between replicates.

Before moving further, it is important to clarify the difference between GSR and burnt SG. Burnt SG is not what is found in crime scenes, which is GSR, a complex mixture that, as mentioned previously, includes burnt propellant particles and even some intact SG particles. Nonetheless, it must be emphasised that it is different to conduct an analysis on burnt SG and on GSR, having different implications. The analysis of burnt SG samples, in this work, served as a precursor and test of the methodology to evaluate if the methods are fit for detecting burnt compounds, compared with intact counterpart. Burning SG will generate new compounds, which are not present in intact samples. However, not all compounds in SG burn when ignited.

Results and Discussion



Chemometric Profile of Gunpowder



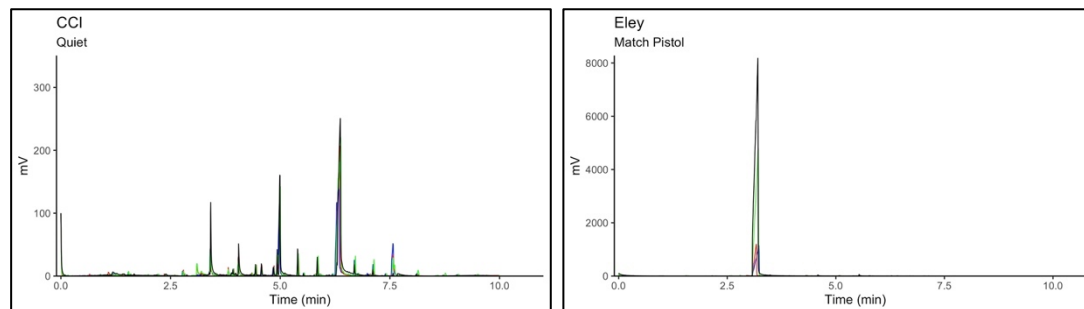


Figure 10 – Normalised SPME/GC-FID chromatograms of intact gunpowder of the 20 analysed samples, with the 4 replicates (RT below the IS peak was removed).

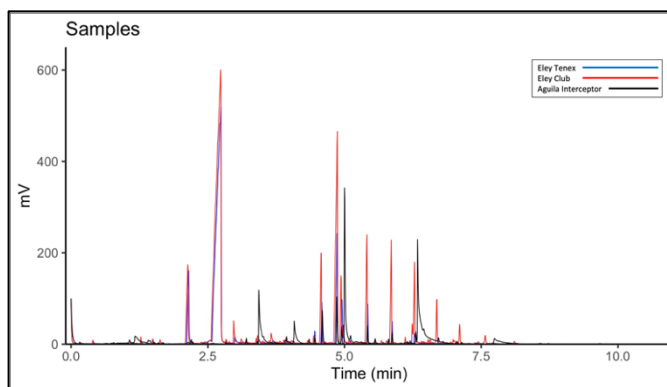
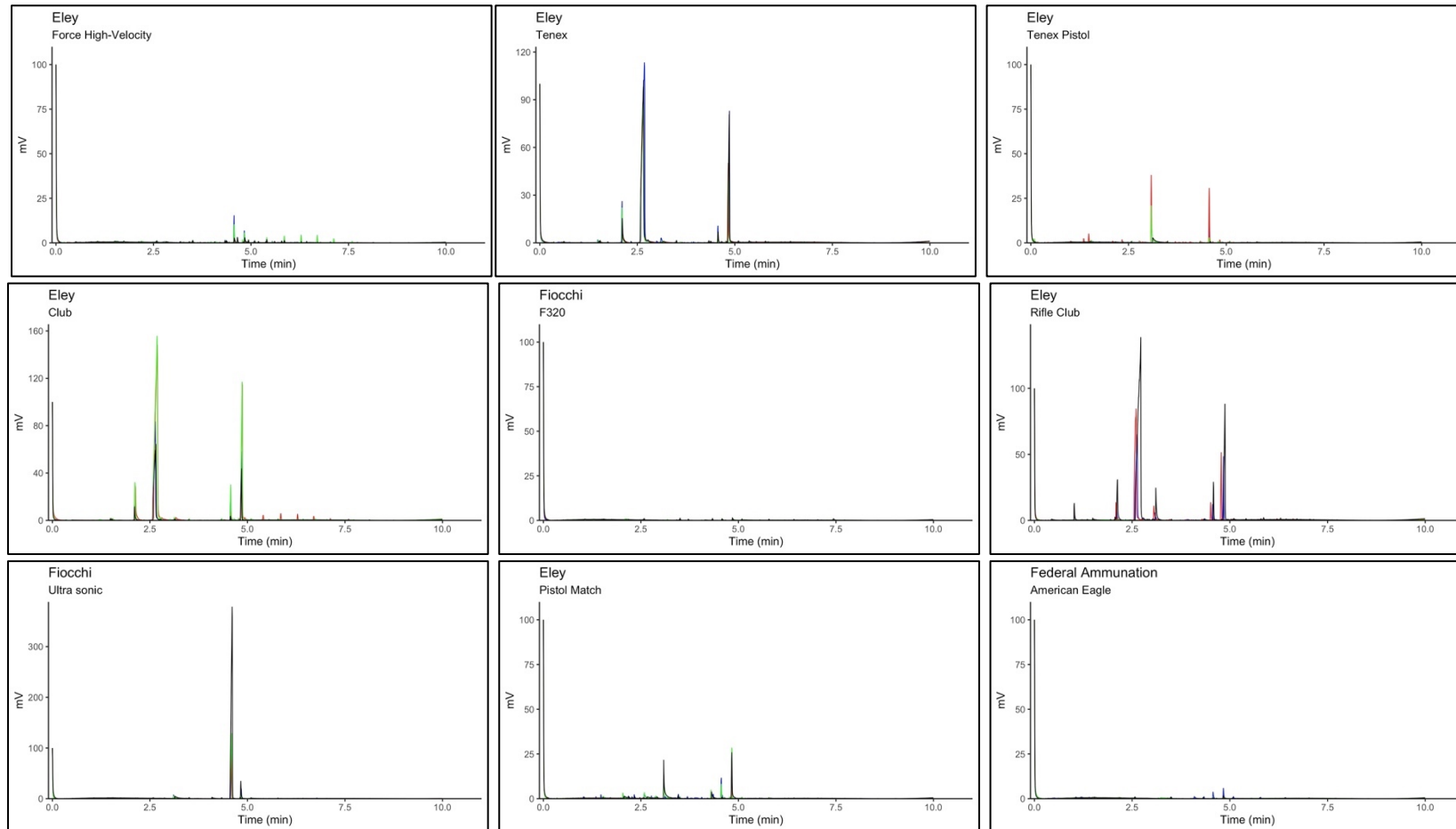
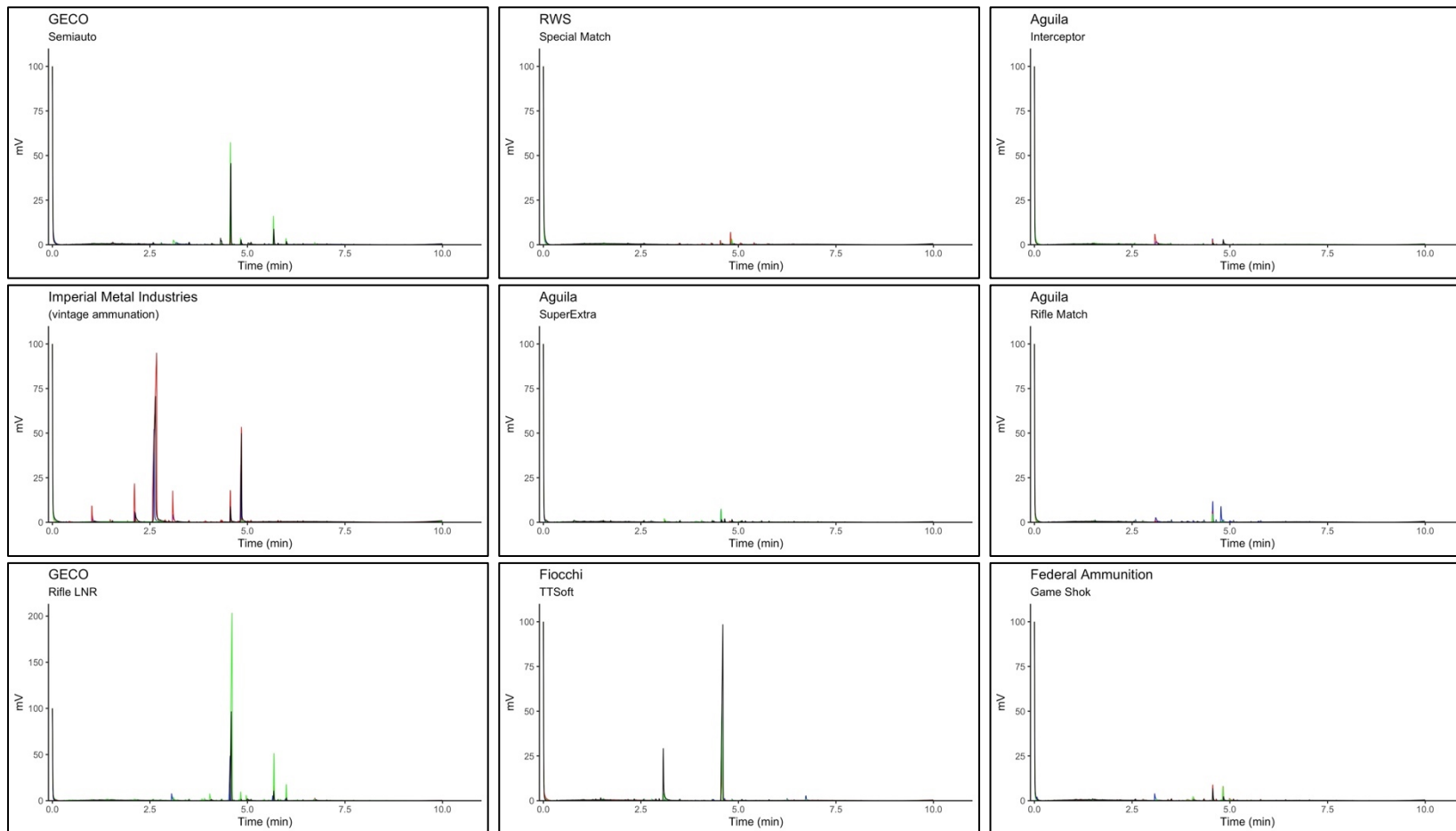


Figure 11 – Normalised SPME/GC-FID Chromatogram of intact SG 3 different samples (ammunition from Eley Tenex, Eley Club and Aguila Interceptor).

Chemometric Profile of Gunpowder



Results and Discussion



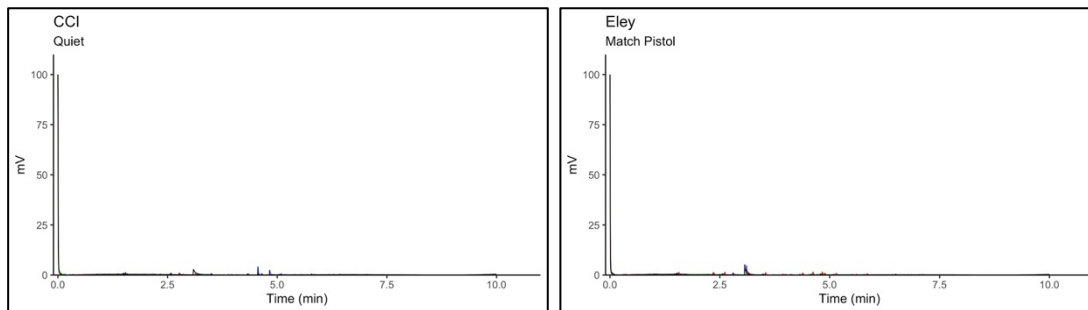


Figure 12 – Normalised SPME/GC-FID chromatograms of burnt gunpowder of the 20 analysed samples, with the 4 replicates (RT below the IS peak was removed).

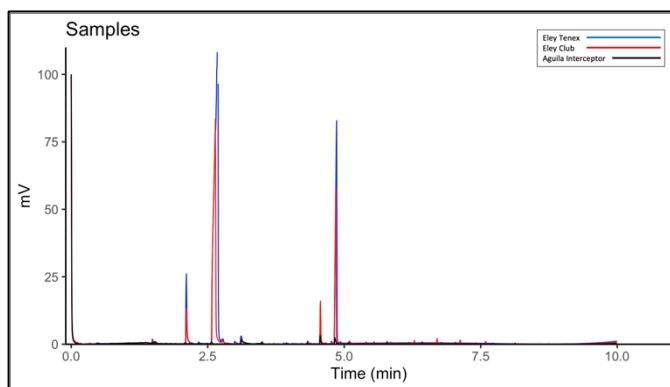


Figure 13 – Normalised SPME/GC-FID Chromatogram of burnt SG 3 different samples (ammunition from Eley Tenex, Eley Club and Aguila Interceptor).

3.4. Training and Validation of the Predictive models

Two classification prediction algorithms were selected, since achieved the best performance results of all the models tested: Random Forests (rf) (164) and C50 (165). The performance of the predictors was evaluated based on the accuracy of training and validation of the models. Both models are based on decision trees, a statistical tool that divides the data in smaller groups, while creating the structure of the tree. The structure of a decision tree includes internal nodes (represents a test applied to an attribute), branches (represents the outcome of the node) and leaves nodes (represents a class) (171). These predictors were chosen based on its easy use and interpretation, their usefulness even with a reduced amount of data. All the models were trained with the same three replicates from each sample, using the function 'train' from 'caret' package (163). The training method included 10 folds and 5 repeats per fold, used to determine the best hyperparameters for the models, with no further pre-processing, apart from mentioned cases, were PCA was also included as an extra pre-processing step in the method's training. All the code referring to these procedures is in Appendix.

Training the predictor using pre-processed chromatographic data achieved better results. The models were trained in two distinct ways: without further pre-processing and using PCA as an extra pre-processing step. A total of 16 different predictive models were trained and evaluated, based on the type of data and model used, as well as additional pre-processing. The accuracy of the training, meaning the accuracy of the model classifying the data on each it was trained, was of 1.00 for all the predictive models developed, as visible in Table 8. This translates in a correct classification of all the samples used in its training.

The validation of the models was evaluated based on the accuracy of the model in classifying the validation data, which consisted of the fourth replicate, not used on the training.

Performance results showed that some models were clearly better than others (Table 8), despite all achieving a accuracy of 100% when subject to the data on which they were trained, the best accuracy of a predictor classifying validation samples was 65%, achieved by RF without extra pre-processing steps when predicting chromatograms of intact SG samples. The same accuracy values were also obtained by the RF classifier with PCA as an extra pre-processing step, when predicting spectra of intact SG samples.

PCA pre-processing seems to decrease the accuracy of decision trees of C5.0 package. The same cannot be affirmed when analysing RF, since the accuracy decreases for intact and burnt SG samples, but increases when predicting spectra, either alone or combined with chromatograms of intact SG samples.

The developed predictors, using spectra and chromatograms of intact SG samples indicates the discriminatory capability of the chemical profiles obtained with these techniques. Combining chromatographic and spectra data seems to be slightly less successful compared when trying to classify samples using only one of these types of data.

The accuracy values expressed on Table 8 may indicate that the model is overfitted for the training data. A model is considered overfitted when it relies on irrelevant features and it is visible when the accuracy of the model when trying to classify data not used in his training is considerably lower than its accuracy when classifying the data on which it was trained (172). This may be related to the low number of samples used for training of the models (172). A solution is the analysis of more replicates, but this is not always possible, as it is expensive and time consuming. So, a data augmentation might help overcome this shortcoming (158,173). A technique of data augmentation is the addition of Gaussian noise (159). This approach was tested initially when working only with the peaks and not the entire chromatogram but have proven less useful when compared with the use of the entire chromatogram. Data augmentation steps are more difficult to implement in an entire chromatogram and did not produce an increase in the accuracy values when the model was attempting to classify new samples, with the accuracy values remaining the same compared to those obtained with the addition of synthetic samples.

Results and Discussion

Table 8- Accuracy of tested predictive models (column “Pre-Process” does not include the pre-process expressed in 3.4.1).

Data used	Model used	Pre-Process	Training Accuracy	Validation Accuracy
Spectra	RF	-	1.00	0.60
Spectra	RF	PCA	1.00	0.65
Spectra	C5.0	-	1.00	0.45
Spectra	C5.0	PCA	1.00	0.35
Intact SG Chromatograms	RF	-	1.00	0.65
Intact SG Chromatograms	RF	PCA	1.00	0.60
Intact SG Chromatograms	C5.0	-	1.00	0.45
Intact SG Chromatograms	C5.0	PCA	1.00	0.35
Burnt SG Chromatograms	RF	-	1.00	0.25
Burnt SG Chromatograms	RF	PCA	1.00	0.10
Burnt SG Chromatograms	C5.0	-	1.00	0.20
Burnt SG Chromatograms	C5.0	PCA	1.00	0.15
Spectra + Intact SG Chromatograms	RF	-	1.00	0.55
Spectra + Intact SG Chromatograms	RF	PCA	1.00	0.60
Spectra + Intact SG Chromatograms	C5.0	-	1.00	0.35
Spectra + Intact SG Chromatograms	C5.0	PCA	1.00	0.35

4. Conclusion

In the present contribution, the chemical profile of several .22 LR ammunition was determined by ATR-FTIR and SPME/GC-FID analysis. This data was used to create predictors to classify samples of SG based on the chemical profile obtained by these techniques.

Alternative analytical methods that include ATR-FTIR and SPME/GC-FID can be helpful in the identification ballistics, particularly for firearm-related elements found in crime scenes where the conventional forensic ballistic visual comparison cannot be used. In addition, these methodologies produce a considerable amount of data that was and is currently driving the exploration of new approaches to answer other vital questions within the field of forensic ballistics. These include the development of predictive models to determine time since shooting and firing distances and, in the case of the present work, to identifying ammunition's manufacturer and its model. This takes advantage of the most recent statistical and machine learning tools currently available for model development and of modern computational database systems for the efficient storage and access to this data.

The results show that the chemical profiles of the analysed SG are clearly different, especially when evaluating the chromatographic data. Nevertheless, the accuracy of the predictor when classifying samples that were not used in its training, was not ideal, showing signs of overfitting. These derives from the data collected and used on the training. The reproducibility of the techniques plays an important part in the predictor success, alongside the limited amount of data. These two factors may have hindered further success of the predictor. In order to improve the model, and subsequently the predictor's accuracy, the data acquisition process should be more reproducible. The use of an automatic SPME apparatus should decrease the deviations on the RT of peaks, and also the use of a second internal standard, with higher mass and non-polar characteristics, that elutes at the end of the chromatographic run, can also assist in data alignment and overall precision. Furthermore, the application of other analytical techniques including RAMAN spectrometry and GC coupled to mass spectrometry, can provide additional information which can improve the accuracy of the predictive model.

The present contribution aimed to fill a void on ammunition control. In Portugal and many other countries, firearms are rigorously controlled and can be traced back to the owner.

However, ammunition records are non-existent since no method to identify ammunition manufacturers and models is in use within Portuguese and other national authorities.

The results and conclusions herein shown can be a precursor for the implementation of ammunition traceability, which will have an impact in forensic ballistics and criminal investigation around the world. The calibre chosen to start is related to the fact that .22 LR ammunition are the most commercially viable ammunition calibre and the most used in short firearms. Nevertheless, the methodology can easily be applied to other calibres and even other types of explosives.

5. Future Perspectives

Steps that can be taken to improve on the developed procedure may include an extra sample preparation step, by fine grinning the intact SG. Adding a second IS solution to the vial could assist in data pre-processing, since it can be used on the second stage of the alignment of the chromatograms. The use of an automatic SPME system can increase reproducibility.

The use of new data pre-processing methods can also improve the predictors. The selection of more relevant features, the increasing of signal/noise ratio and artificial data augmentation can help increase the predictors' performance.

6. References

1. UNODC. Global Firearms Programme [Internet]. 2011. Available from: <https://www.unodc.org/unodc/en/firearms-protocol/index.html>
2. Krüsselmann K, Aarten P, Liem M. Firearms and violence in Europe-A systematic review. Useche SA, editor. PLoS One. 2021 Apr 14;16(4 April).
3. European Parliament, Council of the European Union. Directive (EU) 2021/555 of the European Parliament and of the Council of 24 March 2021 on control of the acquisition and possession of weapons (codification). PE/56/2020/REV/1 EU: L 115/1; 2021 p. 1–25.
4. Institute for Health Metrics and Evaluation (IHME). GBD Results [Internet]. Seattle, WA: IHME, University of Washington: Institute for Health Metrics and Evaluation (IHME); 2019 [cited 2022 Apr 6]. Available from: <https://vizhub.healthdata.org/gbd-results/>
5. Institute for Economics & Peace. Global Peace Index 2020: Measuring Peace in a Complex World. Institute for Economics & Peace. Sydney; 2021.
6. Heard BJ. Handbook of Firearms and Ballistics: Examining and Interpreting Forensic Evidence: Second Edition. Handbook of Firearms and Ballistics: Examining and Interpreting Forensic Evidence: Second Edition. Chichester, UK, UK: John Wiley & Sons, Ltd; 2008. 1–402 p.
7. Smyth Wallace J. Chemical Analysis of Firearms, Ammunition, and Gunshot Residue. Houck M, editor. Chemical Analysis of Firearms, Ammunition, and Gunshot Residue. Boca Raton: CRC Press; 2008.
8. Mattijssen EJAT, Witteman CLM, Berger CEH, Brand NW, Stoel RD. Validity and reliability of forensic firearm examiners. Forensic Sci Int. 2020 Feb;307:110112.
9. Carlucci DE, Jacobson SS, Press CRC. Ballistics: theory and design of guns and ammunition [electronic resource]. Boca Raton: CRC Press; 2008.
10. Gallidabino MD, Weyermann C. Time since last discharge of firearms and spent ammunition elements: state of the art and perspectives. Forensic Sci Int. 2020 Jun;311:110290.

11. Lehman DC. Introduction to forensic science. *Clin Lab Sci*. 2012 Apr 1;25(2):107–8.
12. Blakey LS, Sharples GP, Chana K, Birkett JW. Fate and Behavior of Gunshot Residue—A Review. *J Forensic Sci*. 2018 Jan;63(1):9–19.
13. Maitre M, Kirkbride KP, Horder M, Roux C, Beavis A. Current perspectives in the interpretation of gunshot residues in forensic science: A review. *Forensic Sci Int*. 2017 Jan;270:1–11.
14. Jain B, Yadav P. Vibrational spectroscopy and chemometrics in GSR: review and current trend. *Egypt J Forensic Sci*. 2021 Dec 8;11(1):15.
15. Shrivastava P, Jain VK, Nagpal S. Gunshot residue detection technologies—a review. *Egypt J Forensic Sci*. 2021 Dec 1;11(1):11.
16. Goudsmits E, Sharples GP, Birkett JW. Recent trends in organic gunshot residue analysis. *TrAC - Trends Anal Chem*. 2015 Dec;74:46–57.
17. Dalby O, Butler D, Birkett JW. Analysis of gunshot residue and associated materials - A review. *J Forensic Sci*. 2010 Apr 8;55(4):924–43.
18. Zeichner A. Recent developments in methods of chemical analysis in investigations of firearm-related events. *Anal Bioanal Chem*. 2003 Aug 1;376(8):1178–91.
19. Brożek-Mucha Z. Trends in analysis of gunshot residue for forensic purposes. *Anal Bioanal Chem*. 2017 Oct 28;409(25):5803–11.
20. Chang KH, Jayaprakash PT, Yew CH, Abdullah AFL. Gunshot residue analysis and its evidential values: A review. *Aust J Forensic Sci*. 2013 Mar;45(1):3–23.
21. Saverio Romolo F, Margot P. Identification of gunshot residue: A critical review. *Forensic Sci Int*. 2001 Jun;119(2):195–211.
22. Gallidabino M, Romolo FS, Bylenga K, Weyermann C. Development of a novel headspace sorptive extraction method to study the aging of volatile compounds in spent handgun cartridges. *Anal Chem*. 2014 May 6;86(9):4471–8.
23. Taudte RV, Roux C, Blanes L, Horder M, Kirkbride KP, Beavis A. The development and comparison of collection techniques for inorganic and organic gunshot residues. *Anal Bioanal Chem*. 2016 Apr 12;408(10):2567–76.

References

24. Goudsmits E, Blakey LS, Chana K, Sharples GP, Birkett JW. The analysis of organic and inorganic gunshot residue from a single sample. *Forensic Sci Int*. 2019 Jun;299:168–73.
25. Charles S, Geusens N, Vergalito E, Nys B. Interpol review of gunshot residue 2016–2019. *Forensic Sci Int Synerg*. 2020;2:416–28.
26. Gallidabino M, Weyermann C, Romolo FS, Taroni F. Estimating the time since discharge of spent cartridges: A logical approach for interpreting the evidence. *Sci Justice*. 2013 Mar;53(1):41–8.
27. Rijnders MR, Stamouli A, Bolck A. Comparison of GSR composition occurring at different locations around the firing position. *J Forensic Sci*. 2010 May;55(3):616–23.
28. Schwoeble AJ, Exline DL. Current Methods in Forensic Gunshot Residue Analysis. 1st Editio. *Current Methods in Forensic Gunshot Residue Analysis*. CRC Press; 2000. 192 p.
29. López-Í López M, Bravo JC, García-Ruiz C, Torre M. Diphenylamine and derivatives as predictors of gunpowder age by means of HPLC and statistical models. *Talanta*. 2013 Jan;103:214–20.
30. López-López M, Delgado JJ, García-Ruiz C. Ammunition identification by means of the organic analysis of gunshot residues using Raman spectroscopy. *Anal Chem*. 2012 Apr 17;84(8):3581–5.
31. Scherperel G, Reid GE, Waddell Smith R. Characterization of smokeless powders using nanoelectrospray ionization mass spectrometry (nESI-MS). *Anal Bioanal Chem*. 2009 Aug 26;394(8):2019–28.
32. Redouté Minzière V, Werner D, Schneider D, Manganelli M, Jung B, Weyermann C, et al. Combined Collection and Analysis of Inorganic and Organic Gunshot Residues. *J Forensic Sci*. 2020 Jul 17;65(4):1102–13.
33. Dalby O, Birkett JW. The evaluation of solid phase micro-extraction fibre types for the analysis of organic components in unburned propellant powders. *J Chromatogr A*. 2010 Nov;1217(46):7183–8.
34. Burleson GL, Gonzalez B, Simons K, Yu JCC. Forensic analysis of a single particle of partially burnt gunpowder by solid phase micro-extraction-gas

- chromatography-nitrogen phosphorus detector. *J Chromatogr A*. 2009 May;1216(22):4679–83.
35. Thomas JL, Lincoln D, McCord BR. Separation and Detection of Smokeless Powder Additives by Ultra Performance Liquid Chromatography with Tandem Mass Spectrometry (UPLC/MS/MS). *J Forensic Sci*. 2013 May;58(3):609–15.
 36. Scientific Working Group for Gunshot Residue. Guide for Primer Gunshot Residue Analysis by Scanning Electron Microscopy/Energy Dispersive X-Ray Spectrometry. Swggsr. Cincinnati, OH; 2011. p. 1–100.
 37. Feeney W, Menking-Hoggatt K, Vander Pyl C, Ott CE, Bell S, Arroyo L, et al. Detection of organic and inorganic gunshot residues from hands using complexing agents and LC-MS/MS. *Anal Methods*. 2021;13(27):3024–39.
 38. Garofano L, Capra M, Ferrari F, Bizzaro GP, Di Tullio D, Dell’Olio M, et al. Gunshot residue. Further studies on particles of environmental and occupational origin. *Forensic Sci Int*. 1999 Jul;103(1):1–21.
 39. ASTM International SE 0., Scientific Working Group for Gunshot Residue. ASTM E1588 - 16a Standard Practice for Gunshot Residue Analysis by Scanning Electron Microscopy/Energy Dispersive X-Ray Spectrometry. Vol. 14, Active Standard ASTM E1588. 2011. p. 1–100.
 40. Niewoehner L, Wenz HW, Andrasko J, Beijer R, Gunaratnam L. ENFSI Proficiency Test Program on Identification of GSR by SEM/EDX. *J Forensic Sci*. 2003 Jul;48(4):2002396.
 41. Mou Y, Lakadwar J, Rabalais JW. Evaluation of shooting distance by AFM and FTIR/ATR analysis of GSR. *J Forensic Sci*. 2008 Aug;53(6):1381–6.
 42. Sen P, Panigrahi N, Rao MS, Varier KM, Sen S, Mehta GK. Application of Proton-Induced X-Ray Emission Technique to Gunshot Residue Analyses. *J Forensic Sci*. 1982 Apr;27(2):11487J.
 43. Sharma SP, Lahiri SC. A preliminary investigation into the use of FTIR microscopy as a probe for the identification of bullet entrance holes and the distance of firing. *Sci Justice*. 2009 Sep;49(3):197–204.
 44. Martiny A, Campos APC, Sader MS, Pinto MAL. SEM/EDS analysis and characterization of gunshot residues from Brazilian lead-free ammunition.

References

- Forensic Sci Int. 2008 May;177(1):9–17.
45. Moxnes JF, Jensen TL, Smestad E, Unneberg E, Dullum O. Lead free ammunition without toxic propellant gases. *Propellants, Explos Pyrotech.* 2013 Apr;38(2):255–60.
 46. U.S. Fish and Wildlife Service. 2021-2022 Station-Specific Hunting and Sport Fishing Regulations. 86 FR 48822 USA; 2021 p. 48822–83.
 47. European Commission. Commission Regulation (EU) 2021/57 of 25 January 2021 amending Annex XVII to Regulation (EC) No 1907/2006 of the European Parliament and of the Council concerning the Registration, Evaluation, Authorisation and Restriction of Chemicals (REACH) as regards. *C/2021/318 EU: L 24/19; 2021 p. 19–24.*
 48. Taudte RV, Beavis A, Blanes L, Cole N, Doble P, Roux C. Detection of gunshot residues using mass spectrometry. *Biomed Res Int.* 2014;2014:1–16.
 49. Muller D, Levy A, Vinokurov A, Ravreby M, Shelef R, Wolf E, et al. A novel method for the analysis of discharged smokeless powder residues. *J Forensic Sci.* 2007 Jan;52(1):75–8.
 50. Benito S, Abrego Z, Sánchez A, Unceta N, Goicolea MA, Barrio RJ. Characterization of organic gunshot residues in lead-free ammunition using a new sample collection device for liquid chromatography-quadrupole time-of-flight mass spectrometry. *Forensic Sci Int.* 2015 Jan;246:79–85.
 51. Taudte RV, Roux C, Bishop D, Blanes L, Doble P, Beavis A. Development of a UHPLC method for the detection of organic gunshot residues using artificial neural networks. *Anal Methods.* 2015;7(18):7447–54.
 52. Espinoza EO, Thornton JI. Characterization of Smokeless Gunpowder By Means of Diphenylamine stabilizer and its nitrated derivatives. *Anal Chim Acta.* 1994;288:57–69.
 53. Gassner AL, Weyermann C. LC-MS method development and comparison of sampling materials for the analysis of organic gunshot residues. *Forensic Sci Int.* 2016 Jul;264:47–55.
 54. Laza D, Nys B, Kinder J De, Kirsch-De Mesmaeker A, Moucheron C. Development of a quantitative LC-MS/MS method for the analysis of common

- propellant powder stabilizers in gunshot residue. *J Forensic Sci.* 2007 Jul;52(4):842–50.
55. Arndt J, Bell S, Crookshanks L, Lovejoy M, Oleska C, Tulley T, et al. Preliminary evaluation of the persistence of organic gunshot residue. *Forensic Sci Int.* 2012 Oct;222(1–3):137–45.
56. Zhao M, Zhang S, Yang C, Xu Y, Wen Y, Sun L, et al. Desorption electrospray tandem MS (DESI-MSMS) analysis of methyl centralite and ethyl centralite as gunshot residues on skin and other surfaces. *J Forensic Sci.* 2008 Jul;53(4):807–11.
57. Tong Y, Wu Z, Yang C, Yu J, Zhang X, Yang S, et al. Determination of diphenylamine stabilizer and its nitrated derivatives in smokeless gunpowder using a tandem MS method. *Analyst.* 2001;126(4):480–4.
58. Gallidabino M, Romolo FS, Weyermann C. Characterization of volatile organic gunshot residues in fired handgun cartridges by headspace sorptive extraction. *Anal Bioanal Chem.* 2015 Sep 14;407(23):7123–34.
59. Busky RT, Botcher TR, Sandstrom JL, Erickson JA. Nontoxic, noncorrosive phosphorus-based primer compositions and an ordnance element including the same. United States of America; 8540828, 2012. p. 15pp.
60. Grima M, Butler M, Hanson R, Mohameden A. Firework displays as sources of particles similar to gunshot residue. *Sci Justice.* 2012 Mar;52(1):49–57.
61. Mosher P V., McVicar MJ, Randall ED, Sild EH. Gunshot residue-similar particles produced by fireworks. *J Can Soc Forensic Sci.* 1998 Jan;31(3):157–68.
62. Zeichner A, Levin N. More on the Uniqueness of Gunshot Residue (GSR) Particles. *J Forensic Sci.* 1997 Nov 1;42(6):14255J.
63. Wallace JS, McQuillan J. Discharge Residues from Cartridge-operated Industrial Tools. *J Forensic Sci Soc.* 1984 Sep;24(5):495–508.
64. Torre C, Mattutino G, Vasino V, Robino C. Brake Linings: A Source of Non-GSR Particles Containing Lead, Barium, and Antimony. *J Forensic Sci.* 2002 May;47(3):494–504.
65. Cardinetti B, Ciampini C, D’Onofrio C, Orlando G, Gravina L, Ferrari F, et al. X-

- ray mapping technique: A preliminary study in discriminating gunshot residue particles from aggregates of environmental occupational origin. *Forensic Sci Int.* 2004 Jun;143(1):1–19.
66. Cook M. Gunshot residue contamination of the hands of police officers following start-of-shift handling of their firearm. *Forensic Sci Int.* 2016 Dec;269:56–62.
67. Ali L, Brown K, Castellano H, Wetzel SJ. A Study of the Presence of Gunshot Residue in Pittsburgh Police Stations using SEM/EDS and LC-MS/MS. *J Forensic Sci.* 2016 Jul;61(4):928–38.
68. Lloyd JBF. Diphenylamine Traces in Handwabs and Clothing Debris: Cleanup and Liquid Chromatography with Sequential Oxidative and Reductive Electrochemical Detection. *Anal Chem.* 1987 May 15;59(10):1401–4.
69. Larrañaga MD, Lewis RJ, Lewis RA. *Hawley's Condensed Chemical Dictionary, Sixteenth Edition.* Hawley's Condensed Chemical Dictionary, Sixteenth Edition. Hoboken, NJ, USA: John Wiley & Sons, Inc.; 2016.
70. Pun KM, Gallusser A. Macroscopic observation of the morphological characteristics of the ammunition gunpowder. *Forensic Sci Int.* 2008 Mar;175(2–3):179–85.
71. Chang KH, Jayaprakash PT, Abdullah AFL. Application of different standard loading approaches during solid phase microextraction for forensic analysis of single particle smokeless powders. *Aust J Forensic Sci.* 2015 Apr 3;47(2):147–60.
72. Chang KH, Yew CH, Abdullah AFL. Optimization of headspace solid-phase microextraction technique for extraction of volatile smokeless powder compounds in forensic applications. *J Forensic Sci.* 2014 Jul;59(4):1100–8.
73. Bueno J, Lednev IK. Advanced statistical analysis and discrimination of gunshot residue implementing combined Raman and FT-IR data. *Anal Methods.* 2013;5(22):6292–6.
74. Bueno J, Lednev IK. Raman microspectroscopic chemical mapping and chemometric classification for the identification of gunshot residue on adhesive tape. *Anal Bioanal Chem.* 2014 Jul 17;406(19):4595–9.
75. Bueno J, Sikirzhyski V, Lednev IK. Raman spectroscopic analysis of gunshot residue offering great potential for caliber differentiation. *Anal Chem.* 2012 May

- 15;84(10):4334–9.
76. Vuki M, Shiu KK, Galik M, O'Mahony AM, Wang J. Simultaneous electrochemical measurement of metal and organic propellant constituents of gunshot residues. *Analyst*. 2012;137(14):3265–70.
 77. O'Mahony AM, Wang J. Electrochemical detection of gunshot residue for forensic analysis: A review. *Electroanalysis*. 2013 Jun;25(6):1341–58.
 78. Northrop DM, MacCrehan WA. Smokeless powder residue analysis by capillary electrophoresis. 1997.
 79. Gassner AL, Ribeiro C, Kobylinska J, Zeichner A, Weyermann C. Organic gunshot residues: Observations about sampling and transfer mechanisms. *Forensic Sci Int*. 2016 Sep;266:369–78.
 80. Persin B, Touron P, Mille F, Bernier G, Subercazes T. Évaluation De La Date D'Un Tir. *J Can Soc Forensic Sci*. 2007 Jan;40(2):65–85.
 81. Andrasko J, Stähling S. Time Since Discharge of Pistols and Revolvers. *J Forensic Sci*. 2003 Mar;48(2):2002035.
 82. Wilson JD, Tebow JD, Moline KW. Time Since Discharge of Shotgun Shells. *J Forensic Sci*. 2003 Nov;48(6):2003119.
 83. Serwy IB, Wanderley KA, Lucena MAM, Maldaner AO, Talhavini M, Rodrigues MO, et al. [Ln₂(BDC)₃(H₂O)₄]_n: A low cost alternative for GSR luminescent marking. *J Lumin*. 2018 Aug;200:24–9.
 84. Filho EV, de Sousa Filho PC, Serra OA, Weber IT, Lucena MAM, Luz PP. New luminescent lanthanide-based coordination compounds: Synthesis, studies of optical properties and application as marker for gunshot residues. *J Lumin*. 2018 Oct;202(May):89–96.
 85. Weber IT, Melo AJG, Lucena MAM, Consoli EF, Rodrigues MO, de Sá GF, et al. Use of luminescent gunshot residues markers in forensic context. *Forensic Sci Int*. 2014 Nov;244:276–84.
 86. Weber IT, De Melo AJG, Lucena MADM, Rodrigues MO, Alves Junior S. High photoluminescent metal - Organic frameworks as optical markers for the identification of gunshot residues. *Anal Chem*. 2011 Jun 15;83(12):4720–3.

References

87. Lucena MAM, Oliveira MFL, Arouca AM, Talhavini M, Ferreira EA, Alves S, et al. Application of the Metal-Organic Framework [Eu(BTC)] as a Luminescent Marker for Gunshot Residues: A Synthesis, Characterization, and Toxicity Study. *ACS Appl Mater Interfaces*. 2017 Feb 8;9(5):4684–91.
88. Albino de Carvalho M, Talhavini M, Pimentel MF, Amigo JM, Pasquini C, Junior SA, et al. NIR hyperspectral images for identification of gunshot residue from tagged ammunition. *Anal Methods*. 2018;10(38):4711–7.
89. Melo Lucena MA, Rodrigues MO, Gatto CC, Talhavini M, Maldaner AO, Alves S, et al. Synthesis of [Dy(DPA)(HDP)] and its potential as gunshot residue marker. *J Lumin*. 2016 Feb;170:697–700.
90. Destefani CA, Motta LC, Vanini G, Souza LM, Filho JFA, Macrino CJ, et al. Europium-organic complex as luminescent marker for the visual identification of gunshot residue and characterization by electrospray ionization FT-ICR mass spectrometry. *Microchem J*. 2014 Sep;116:216–24.
91. Chang KH, Abdullah AFL. A Review on Solid Phase Microextraction and Its Applications in Gunshot Residue Analysis. *Malaysian J Forensic Sci*. 2010;1(1):42–7.
92. Fitsev IM, Blokhin VK, Budnikov GK. Chromatographic techniques in forensic chemical examinations. *Zhurnal Anal Khimii*. 2004;59(12):1289–98.
93. Dufour E. Chapter 1 - Principles of Infrared Spectroscopy. In: *Infrared Spectroscopy for Food Quality Analysis and Control*. Elsevier; 2009. p. 1–27.
94. Subramanian A, Rodriguez-Saona L. Chapter 7 - Fourier Transform Infrared (FTIR) Spectroscopy. In: *Infrared Spectroscopy for Food Quality Analysis and Control*. Elsevier; 2009.
95. Larkin P. Chapter 3 - Instrumentation and Sampling Methods. In: *Infrared and Raman Spectroscopy*. Elsevier; 2011. p. 27–54.
96. Ferrer N. Forensic Science, Applications of Infrared Spectroscopy. In: *Reference Module in Chemistry, Molecular Sciences and Chemical Engineering*. Elsevier; 2014.
97. Bueno J, Lednev IK. Attenuated total reflectance-FT-IR imaging for rapid and automated detection of gunshot residue. *Anal Chem*. 2014 Apr 1;86(7):3389–96.

98. Lo TC, Baird MHI. Solvent Extraction. In: Meyers RA, editor. *Encyclopedia of Physical Science and Technology*. 3rd ed. Tarzana, California, USA: Elsevier; 2001. p. 341–62.
99. de Perre C, Corbin I, Blas M, McCord BR. Separation and identification of smokeless gunpowder additives by capillary electrochromatography. *J Chromatogr A*. 2012 Dec;1267:259–65.
100. Zeichner A, Eldar B. A Novel Method for Extraction and Analysis of Gunpowder Residues on Double-Side Adhesive Coated Stubs. *J Forensic Sci*. 2004 Nov;49(6):1–13.
101. López-López M, de la Ossa MÁF, Galindo JS, Ferrando JL, Vega A, Torre M, et al. New protocol for the isolation of nitrocellulose from gunpowders: Utility in their identification. *Talanta*. 2010;81(4–5):1742–9.
102. Fryš O, BajeroVá P, Eisner A, Mudruňková M, Ventura K. Method validation for the determination of propellant components by Soxhlet extraction and gas chromatography/mass spectrometry. *J Sep Sci*. 2011 Sep;34(18):2405–10.
103. López-López M, Merk V, García-Ruiz C, Kneipp J. Surface-enhanced Raman spectroscopy for the analysis of smokeless gunpowders and macroscopic gunshot residues. *Anal Bioanal Chem*. 2016 Jul 30;408(18):4965–73.
104. Zeichner A, Eldar B, Glattstein B, Koffman A, Tamiri T, Muller D. Vacuum Collection of Gunpowder Residues from Clothing Worn by Shooting Suspects, and Their Analysis by GC/TEA, IMS, and GC/MS. *J Forensic Sci*. 2003 Sep;48(5):2002390.
105. Sauzier G, Bors D, Ash J, Goodpaster J V., Lewis SW. Optimisation of recovery protocols for double-base smokeless powder residues analysed by total vaporisation (TV) SPME/GC-MS. *Talanta*. 2016 Sep;158:368–74.
106. Weyermann C, Belaud V, Riva F, Romolo FS. Analysis of organic volatile residues in 9 mm spent cartridges. *Forensic Sci Int*. 2009;186(1–3):29–35.
107. Andrasko J, Stähling S. Time Since Discharge of Rifles. *J Forensic Sci*. 2000 Nov;45(6):14874J.
108. Joshi M, Rigsby K, Almirall JR. Analysis of the headspace composition of smokeless powders using GC-MS, GC- μ ECD and ion mobility spectrometry.

References

- Forensic Sci Int. 2011 May;208(1–3):29–36.
109. Furton KG, Almirall JR, Bi M, Wang J, Wu L. Application of solid-phase microextraction to the recovery of explosives and ignitable liquid residues from forensic specimens. *J Chromatogr A*. 2000 Jul;885(1–2):419–32.
 110. Pert AD, Baron MG, Birkett JW. Review of analytical techniques for arson residues. *J Forensic Sci*. 2006 Sep;51(5):1033–49.
 111. Chang KH, Abdullah AFL. Extraction Efficiency of the Sequential Solid Phase Microextraction of Gunshot Residues from Spent Cartridges. *Malaysian J Forensic Sci J Forensic Sci*. 2014;5(1):7–11.
 112. Gallidabino M, Romolo FS, Weyermann C. Time since discharge of 9 mm cartridges by headspace analysis, part 1: Comprehensive optimisation and validation of a headspace sorptive extraction (HSSE) method. *Forensic Sci Int*. 2017 Mar;272:159–70.
 113. Gallidabino M, Romolo FS, Weyermann C. Time since discharge of 9 mm cartridges by headspace analysis, part 2: Ageing study and estimation of the time since discharge using multivariate regression. *Forensic Sci Int*. 2017 Mar;272:171–83.
 114. Tienpont B, David F, Bicchi C, Sandra P. High capacity headspace sorptive extraction. *J Microcolumn Sep*. 2000;12(11):577–84.
 115. Farber C, Li J, Hager E, Chemelewski R, Mullet J, Rogachev AY, et al. Complementarity of Raman and Infrared Spectroscopy for Structural Characterization of Plant Epicuticular Waxes. *ACS Omega*. 2019 Feb 28;4(2):3700–7.
 116. López-López M, Ferrando JL, García-Ruiz C. Comparative analysis of smokeless gunpowders by Fourier transform infrared and Raman spectroscopy. *Anal Chim Acta*. 2012 Mar;717:92–9.
 117. Griffiths PR, de Haseth JA. *Fourier Transform Infrared Spectrometry*. 2nd ed. Hoboken, NJ, USA: John Wiley & Sons, Inc.; 2007. 1–55 p.
 118. Hammes GG. *Spectroscopy for the Biological Sciences*. Hoboken, NJ, USA: John Wiley & Sons, Inc.; 2005.

119. White R. *Chromatography/Fourier Transform Infrared Spectroscopy and Its Applications*. 10th ed. CRC Press; 2020.
120. Schrader B. *Infrared and Raman Spectroscopy: Methods and Applications*. New York: Weinheim; 2008. 787 p.
121. Lee LC, Liong CY, Jemain AA. A contemporary review on Data Preprocessing (DP) practice strategy in ATR-FTIR spectrum. *Chemom Intell Lab Syst*. 2017 Apr;163(February):64–75.
122. Zhang J, Li B, Wang Q, Li C, Zhang Y, Lin H, et al. Characterization of postmortem biochemical changes in rabbit plasma using ATR-FTIR combined with chemometrics: A preliminary study. *Spectrochim Acta - Part A Mol Biomol Spectrosc*. 2017 Feb;173:733–9.
123. ANDERSON JM, VOSKERICIAN G. The challenge of biocompatibility evaluation of biocomposites. In: *Biomedical Composites*. Elsevier; 2010. p. 325–53.
124. Brożek-Mucha Z. A study of gunshot residue distribution for close-range shots with a silenced gun using optical and scanning electron microscopy, X-ray microanalysis and infrared spectroscopy. *Sci Justice*. 2017 Mar;57(2):87–94.
125. Sharma SP, Lahiri SC. Characterization and identification of explosives and explosive residues using GC-MS, an FTIR microscope, and HPTLC. *J Energ Mater*. 2005 Oct;23(4):239–64.
126. Bueno J, Sikirzhytski V, Lednev IK. Attenuated total reflectance-FT-IR spectroscopy for gunshot residue analysis: Potential for ammunition determination. *Anal Chem*. 2013 Aug 6;85(15):7287–94.
127. Gardiner DJ, Graves PR. *Practical Raman Spectroscopy*. Gardiner DJ, Graves PR, editors. Berlin, Heidelberg: Springer Berlin Heidelberg; 1989. 1–76 p.
128. Atkins P, de Paula J. *Elements of physical chemistry*. 5th ed. Oxford: Oxford U.P.; 2009. 459 p.
129. Abrego Z, Grijalba N, Unceta N, Maguregui M, Sanchez A, Fernández-Isla A, et al. A novel method for the identification of inorganic and organic gunshot residue particles of lead-free ammunitions from the hands of shooters using scanning laser ablation-ICPMS and Raman micro-spectroscopy. *Analyst*. 2014;139(23):6232–41.

References

130. Chaves das Neves HJ, Costa Freitas AM. Introdução à cromatografia gás-líquido de alta resolução. Dias de Sousa L, editor. Póvoa de Santa Iria - Portugal; 1996.
131. Moran JW, Bell S. Skin permeation of organic gunshot residue: Implications for sampling and analysis. *Anal Chem*. 2014 Jun 17;86(12):6071–9.
132. Cascio O, Trettene M, Bortolotti F, Milana G, Tagliaro F. Analysis of organic components of smokeless gunpowders: High-performance liquid chromatography vs. micellar electrokinetic capillary chromatography. *Electrophoresis*. 2004 Jun;25(10–11):1543–7.
133. Lussier LS, Gagnon H, Bohn MA. On the chemical reactions of diphenylamine and its derivatives with nitrogen dioxide at normal storage temperature conditions. *Propellants, Explos Pyrotech*. 2000 Jun;25(3):117–25.
134. Chajistamatiou AS, Bakeas EB. A rapid method for the identification of nitrocellulose in high explosives and smokeless powders using GC-EI-MS. *Talanta*. 2016 May;151:192–201.
135. Joshi M, Delgado Y, Guerra P, Lai H, Almirall JR. Detection of odor signatures of smokeless powders using solid phase microextraction coupled to an ion mobility spectrometer. *Forensic Sci Int*. 2009 Jul;188(1–3):112–8.
136. Chang KH, Yew CH, Abdullah AFL. Study of the Behaviors of Gunshot Residues from Spent Cartridges by Headspace Solid-Phase Microextraction-Gas Chromatographic Techniques. *J Forensic Sci*. 2015 Jul;60(4):869–77.
137. Tarifa A, Almirall JR. Fast detection and characterization of organic and inorganic gunshot residues on the hands of suspects by CMV-GC-MS and LIBS. *Sci Justice*. 2015 May;55(3):168–75.
138. Cook GW, LaPuma PT, Hook GL, Eckenrode BA. Using gas chromatography with ion mobility spectrometry to resolve explosive compounds in the presence of interferences. *J Forensic Sci*. 2010 Nov;55(6):1582–91.
139. Sauzier G, Van Bronswijk W, Lewis SW. Chemometrics in forensic science: Approaches and applications. *Analyst*. 2021;146(8):2415–48.
140. Rohman A, Ghazali MAIB, Windarsih A, Irnawati, Riyanto S, Yusof FM, et al. Comprehensive Review on Application of FTIR Spectroscopy Coupled with Chemometrics for Authentication Analysis of Fats and Oils in the Food Products.

- Molecules. 2020 Nov 23;25(22):54–85.
141. Tortorella S, Cinti S. How Can Chemometrics Support the Development of Point of Need Devices? *Anal Chem.* 2021;93(5):2713–22.
 142. Ziegel ER. Statistics and Chemometrics for Analytical Chemistry. *Technometrics.* 2004 Nov;46(4):498–9.
 143. Gosav S, Praisler M, Van Bocxlaer J, De Leenheer AP, Massart DL. Class identity assignment for amphetamines using neural networks and GC-FTIR data. *Spectrochim Acta - Part A Mol Biomol Spectrosc.* 2006 Aug;64(5):1110–7.
 144. Friedman JH. Multivariate Adaptive Regression Splines. *Ann Stat.* 1991 Mar 1;19(1).
 145. Bell S, Seitzinger L. From binary presumptive assays to probabilistic assessments: Differentiation of shooters from non-shooters using IMS, OGSR, neural networks, and likelihood ratios. *Forensic Sci Int.* 2016 Jun;263:176–85.
 146. Wold S, Sjöström M, Eriksson L. PLS-regression: a basic tool of chemometrics. *Chemom Intell Lab Syst.* 2001 Oct;58(2):109–30.
 147. Costa C, Maraschin M, Rocha M. An R package for the integrated analysis of metabolomics and spectral data. *Comput Methods Programs Biomed.* 2016 Jun;129:117–24.
 148. Bro R, Smilde AK. Principal component analysis. *Anal Methods.* 2014;6(9):2812–31.
 149. Nielsen F. Hierarchical Clustering. In: *Introduction to HPC with MPI for Data Science.* 2016. p. 195–211.
 150. Ruiz-Perez D, Guan H, Madhivanan P, Mathee K, Narasimhan G. So you think you can PLS-DA? *BMC Bioinformatics.* 2020 Dec 9;21(S1):2.
 151. Lee LC, Liong C-Y, Jemain AA. Partial least squares-discriminant analysis (PLS-DA) for classification of high-dimensional (HD) data: a review of contemporary practice strategies and knowledge gaps. *Analyst.* 2018;143(15):3526–39.
 152. Hastie T, Tibshirani R, Friedman J. *The Elements of Statistical Learning.* New York, NY: Springer New York; 2009. 321–328 p. (Springer Series in Statistics).
 153. Jolliffe IT, Cadima J. Principal component analysis: a review and recent

References

- developments. *Philos Trans R Soc A Math Phys Eng Sci.* 2016 Apr 13;374(2065):20150202.
154. Taunk K, De S, Verma S, Swetapadma A. A Brief Review of Nearest Neighbor Algorithm for Learning and Classification. In: 2019 International Conference on Intelligent Computing and Control Systems (ICCS). IEEE; 2019. p. 1255–60.
155. Cortes C, Vapnik V. Support-vector networks. *Mach Learn.* 1995 Sep;20(3):273–97.
156. Reese KL, Jones AD, Smith RW. Characterization of smokeless powders using multiplexed collision-induced dissociation mass spectrometry and chemometric procedures. *Forensic Sci Int.* 2017 Mar;272:16–27.
157. Georgouli K, Osorio MT, Martinez Del Rincon J, Koidis A. Data augmentation in food science: Synthesising spectroscopic data of vegetable oils for performance enhancement. *J Chemom.* 2018 Jun;32(6):e3004.
158. Dyk DAV, Meng XL. The art of data augmentation. *J Comput Graph Stat.* 2001 Jul 26;10(1):1–50.
159. Conlin AK, Martin EB, Morris AJ. Data augmentation: An alternative approach to the analysis of spectroscopic data. *Chemom Intell Lab Syst.* 1998 Dec;44(1–2):161–73.
160. Wrobel HA, Millar MJ, Kijek M. Identification of Ammunition from Gunshot Residues and Other Cartridge Related Materials—A Preliminary Model Using .22 Caliber Rimfire Ammunition. *J Forensic Sci.* 1998;43(2):16141J.
161. Liland KH, Almøy T, Mevik B-H. Optimal Choice of Baseline Correction for Multivariate Calibration of Spectra. *Appl Spectrosc.* 2010 Sep 1;64(9):1007–16.
162. Wickham H. *ggplot2: Elegant Graphics for Data Analysis.* Springer-Verlag New York; 2016.
163. Kuhn M. *caret: Classification and Regression Training.* 2022.
164. Liaw A, Wiener M. Classification and Regression by randomForest. *R News.* 2002;2(3):18–22.
165. Kuhn M, Quinlan R. *C50: C5.0 Decision Trees and Rule-Based Models.* 2022.
166. Nakanishi K, Solomon P. *Infrared Absorption Spectroscopy.* San Francisco:

Holden-Day, Inc.; 1977.

167. Smith B. *Infrared Spectral Interpretation*. New York: CRC; 1999.
168. Kovalenko VI, Mukhamadeeva RM, Maklakova LN, Gustova NG. Interpretation of the IR spectrum and structure of cellulose nitrate. *J Struct Chem*. 1994;34(4):540–7.
169. Pellati F, Benvenuti S, Yoshizaki F, Bertelli D, Rossi MC. Headspace solid-phase microextraction-gas chromatography–mass spectrometry analysis of the volatile compounds of *Evodia* species fruits. *J Chromatogr A*. 2005 Sep;1087(1–2):265–73.
170. Carasek E, Pawliszyn J. Screening of Tropical Fruit Volatile Compounds Using Solid-Phase Microextraction (SPME) Fibers and Internally Cooled SPME Fiber. *J Agric Food Chem*. 2006 Nov 1;54(23):8688–96.
171. Kamiński B, Jakubczyk M, Szufel P. A framework for sensitivity analysis of decision trees. *Cent Eur J Oper Res*. 2018 Mar 24;26(1):135–59.
172. Bramer M. Avoiding Overfitting of Decision Trees. In: *Principles of Data Mining*. London: Springer London; 2007. p. 119–34.
173. van Dyk DA, Meng X-L. The Art of Data Augmentation. *J Comput Graph Stat*. 2001 Jul 26;10(1):1–50.

7. Appendix

Spectra Analysis

```

1 # Clean environment
2 rm(list=ls())
3 cat("\14")
4
5 # Load auxiliary functions and libraries
6 source("scripts/functions.R")
7 source("scripts/libraries.R")
8
9 # Data pre-processing
10 ## Load Data
11 ### Run for new data and/or trim (loads and saves data on a .RData file)
12 spectra <- read.spectra('data/ftir/transmittance', trim = c(1800, 550))
13 save(spectra, file = 'Data/intact.gunpowder.ftir.spectra.RData')
14 ### Run subsequently after R object is saved
15 load(file = 'Data/intact.gunpowder.ftir.spectra.RData')
16
17 ## Spectra Normalization
18 spectra.n <- spectra
19 for(nm in names(spectra.n)){
20   max <- max(spectra.n[[nm]]$Transmittance)
21   min <- min(spectra.n[[nm]]$Transmittance)
22   spectra.n[[nm]]$Transmittance <- ((spectra.n[[nm]]$Transmittance - min) / (max - min)) * 100
23 }
24
25 # Predictor
26 ## Setup data frame
27 spct <- data.frame(Wavenumber = spectra.n$A1$Wavenumber)
28 for(nm in names(spectra.n)){
29   spct[[nm]] <- spectra.n[[nm]]$Transmittance
30 }
31
32 ## Input data frame
33 spct.df <- as.data.frame(t(spct[, -1]))
34 colnames(spct.df) <- paste('T', spct$Wavenumber, sep = '')
35 spct.df['Target'] <- as.factor(gsub('\d', '', colnames(spct)[-1]))
36 spct.df['Replicate'] <- gsub('[A-Z]', '', colnames(spct)[-1])
37
38 save(spct.df, spectra.n, file = 'Data/FTIR.predictor_dfs.RData')
39
40 ## Data Division
41 ### Training Data
42 spct.trn <- spct.df[which(spct.df$Replicate == 1 | spct.df$Replicate == 4 | spct.df$Replicate == 3),]
43 x <- spct.trn[, which(colnames(spct.trn) == "Target" | colnames(spct.trn) == "Replicate")]
44 y <- spct.trn[, "Target"]
45
46 ## Model Training without extra pre-processing
47 ### Random Forests
48 set.seed(123)
49 mdl.raw.rf <- train(x, y,
50                   method = 'rf',
51                   trControl = trnctrl)
52
53 ### C5.0
54 set.seed(123)
55 mdl.raw.C50 <- train(x, y,
56                   method = 'C5.0',
57                   trControl = trnctrl)
58
59 ## Predictor Evaluation
60 ### Random Forests
61 confusionMatrix(predict(mdl.raw.rf), y)
62 confusionMatrix(predict(mdl.raw.rf, x.vld), y.vld)
63
64 ### C5.0
65 confusionMatrix(predict(mdl.raw.C50), y)
66 confusionMatrix(predict(mdl.raw.C50, x.vld), y.vld)
67
68 ## Model Training with PCA pre-processing
69 ### Random Forests
70 set.seed(123)
71 mdl.pca.rf <- train(x, y,
72                   method = 'rf',
73                   trControl = trnctrl,
74                   preProcess = c('pca'))
75
76 ### C5.0
77 set.seed(123)
78 mdl.pca.C50 <- train(x, y,
79                   method = 'C5.0',
80                   trControl = trnctrl,
81                   preProcess = c('pca'))
82
83 ## Predictor Evaluation
84 ### Random Forests
85 confusionMatrix(predict(mdl.pca.rf), y)
86 confusionMatrix(predict(mdl.pca.rf, x.vld), y.vld)
87
88 ### C5.0
89 confusionMatrix(predict(mdl.pca.C50), y)
90 confusionMatrix(predict(mdl.pca.C50, x.vld), y.vld)

```

Intact Chromatogram Analysis

```

1 # Clean environment
2 rm(list=ls())
3 cat("\14")
4
5 # Load auxiliary functions and libraries
6 source("scripts/functions.R")
7 source("scripts/libraries.R")
8
9 # Data pre-processing
10 ## Load Data
11 ### Run for new data and/or trim (loads and saves data on a .RData file)
12 chromatograms <- read.chromatograms('data/gc/raw/intact', trim = c(10,22))
13 save(chromatograms, file = 'Data/intact.gunpowder.gc.chromatograms.RData')
14 ### Run subsequently after R object is saved
15 load(file = 'Data/intact.gunpowder.gc.chromatograms.R')
16
17 ## Data Alignment
18 ### Alignment by the IS peak
19 #### Identification of the IS peak
20 drift <- c()
21 for(i in 1:length(chromatograms)){
22   print(names(chromatograms)[i])
23   drift <- c(drift, zero.alignment(chromatograms[[i]]))
24 }
25
26 #### Correction of the RT by the RT(IS)
27 load(file = 'Data/intact.IS.Drift.RData')
28 for(i in 1:length(chromatograms)){
29   chromatograms[[i]]$Time <- chromatograms[[i]]$Time - drift[i]
30 }
31
32 ## Alignment by the last peak pair
33 #### Identification the last pair of peaks
34 stretch <- c()
35 for(i in 1:length(chromatograms)){
36   print(names(chromatograms)[i])
37   stretch <- c(stretch, stretch.alignment(chromatograms$A1, chromatograms[[i]]))
38 }
39
40 ## Correction of the RT by the pair of peaks
41 for(i in 1:length(chromatograms)){
42   chromatograms[[i]]$Time <- chromatograms[[i]]$Time * stretch[i]
43 }
44
45 ## Resolution Reduction
46 chromatograms.rr <- list()
47 for(nm in names(chromatograms)){
48   chromatograms.rr[[nm]] <- resolution.reduction(chromatograms[[nm]])
49 }
50
51 ## Trim data (removes peaks before IS)
52 for (nm in names(chromatograms.rr)) {
53   c <- c()
54   c <- which(chromatograms.rr[[nm]]$Time < 0 | chromatograms.rr[[nm]]$Time >= 10)
55   chromatograms.rr[[nm]] <- chromatograms.rr[[nm]][-c,]
56 }
57
58 ## Baseline Correction
59 chrm.rr.bsl <- subtract.baseline.batch(chromatograms.rr, choose = F, degree = 10)
60
61 ## Normalization
62 for(nm in names(chrm.rr.bsl)){
63   a <- which(chrm.rr.bsl[[nm]]$Time == 0)
64   chrm.rr.bsl[[nm]]$mV <- (chrm.rr.bsl[[nm]]$mV / chrm.rr.bsl[[nm]]$mV[a]) * 100
65 }
66
67 # Predictor
68 ## Setup data frame
69 chrm <- data.frame(Time = chrm.rr.bsl$A1$Time)
70 for(nm in names(chrm.rr.bsl)){
71   chrm[[nm]] <- chrm.rr.bsl[[nm]]$mV
72 }
73

```

```

74 ## Input data frame
75 chrM.df <- as.data.frame(t(chrM[, -1]))
76 colnames(chrM.df) <- paste('T', chrM$time, sep = '')
77 chrM.df['Target'] <- as.factor(gsub('\d', '', colnames(chrM)[-1]))
78 chrM.df['Replicate'] <- gsub('[A-Z]', '', colnames(chrM)[-1])
79
80 ## Data Division
81 ### Training Data
82 chrM.trn <- chrM.df[which(chrM.df$Replicate == 1 | chrM.df$Replicate == 3 | chrM.df$Replicate == 4),]
83 x <- chrM.trn[, -which(colnames(chrM.trn) == "Target" | colnames(chrM.trn) == "Replicate" | colnames(chrM.trn) == 'T0')]
84 y <- chrM.trn[, "Target"]
85
86 ### Validation Data
87 chrM.vld <- chrM.df[which(chrM.df$Replicate == 2),]
88 x.vld <- spct.vld[, -which(colnames(spct.vld) == "Target" | colnames(spct.vld) == "Replicate")]
89 y.vld <- spct.vld[, "Target"]
90
91 ## Predictor Setup
92 ### Model train
93 trnctrl <- trainControl(method = "repeatedcv",
94                       number = 10,
95                       repeats = 5,
96                       verboseIter = T)
97
98 ## Model Training without extra pre-processing
99 ### Random Forests
100 set.seed(123)
101 mdl.raw.rf <- train(x, y,
102                  method = 'rf',
103                  trControl = trnctrl)
104 ### C5.0
105 set.seed(123)
106 mdl.raw.C50 <- train(x, y,
107                   method = 'C5.0',
108                   trControl = trnctrl)
109
110 ## Predictor Evaluation
111 ### Random Forests
112 confusionMatrix(predict(mdl.raw.rf), y)
113 confusionMatrix(predict(mdl.raw.rf, x.vld), y.vld)
114
115 ### C5.0
116 confusionMatrix(predict(mdl.raw.C50), y)
117 confusionMatrix(predict(mdl.raw.C50, x.vld), y.vld)
118
119 ## Model Training with PCA pre-processing
120 ### Random Forests
121 set.seed(123)
122 mdl.pca.rf <- train(x, y,
123                  method = 'rf',
124                  trControl = trnctrl,
125                  preProcess = c('pca'))
126 ### C5.0
127 set.seed(123)
128 mdl.pca.C50 <- train(x, y,
129                   method = 'C5.0',
130                   trControl = trnctrl,
131                   preProcess = c('pca'))
132
133 ## Predictor Evaluation
134 ### Random Forests
135 confusionMatrix(predict(mdl.pca.rf), y)
136 confusionMatrix(predict(mdl.pca.rf, x.vld), y.vld)
137
138 ### C5.0
139 confusionMatrix(predict(mdl.pca.C50), y)
140 confusionMatrix(predict(mdl.pca.C50, x.vld), y.vld)

```

Burnt Chromatogram Analysis

```

1 # Clean environment
2 rm(list=ls())
3 cat("\14")
4
5 # Load auxiliary functions and libraries
6 source("scripts/functions.R")
7 source("scripts/libraries.R")
8
9 # Data pre-processing
10 ## Load Data
11 ### Run for new data and/or trim (loads and saves data on a .RData file)
12 chromatograms <- read.chromatograms('data/gc/raw/burnt', trim = c(10,22))
13 save(chromatograms, file = 'Data/burnt.gunpowder.gc.chromatograms.RData')
14 ### Run subsequently after R object is saved
15 load(file = 'Data/burnt.gunpowder.gc.chromatograms.RData')
16
17 ## Data Alignment
18 ### Alignment by the IS peak
19 #### Identification of the IS peak
20 drift <- c()
21 for(i in 1:length(chromatograms)){
22   print(names(chromatograms)[i])
23   drift <- c(drift, zero.alignment(chromatograms[[i]]))
24 }
25
26 #### Correction of the RT by the RT(IS)
27 load(file = 'Data/burnt.IS_Drift.RData')
28 for(i in 1:length(chromatograms)){
29   chromatograms[[i]]$Time <- chromatograms[[i]]$Time - drift[i]
30 }
31
32 ## Alignment by the last peak pair
33 #### Identification the last pair of peaks
34 stretch <- c()
35 for(i in 1:length(chromatograms)){
36   print(names(chromatograms)[i])
37   stretch <- c(stretch, stretch.alignment(chromatograms$A1, chromatograms[[i]]))
38 }
39
40 ### Correction of the RT by the pair of peaks
41 for(i in 1:length(chromatograms)){
42   chromatograms[[i]]$Time <- chromatograms[[i]]$Time * stretch[i]
43 }
44
45 ## Resolution Reduction
46 chromatograms.rr <- list()
47 for(nm in names(chromatograms)){
48   chromatograms.rr[[nm]] <- resolution.reduction(chromatograms[[nm]])
49 }
50
51 ### Trim data (removes peaks before IS)
52 for (nm in names(chromatograms.rr)) {
53   c <- c()
54   c <- which(chromatograms.rr[[nm]]$Time < 0 | chromatograms.rr[[nm]]$Time >= 10)
55   chromatograms.rr[[nm]] <- chromatograms.rr[[nm]][-c,]
56 }
57
58 ## Baseline Correction
59 chm.rr.bsl <- subtract.baseline.batch(chromatograms.rr, choose = F, degree = 5)
60
61 ## Normalization
62 for(nm in names(chm.rr.bsl)){
63   a <- which(chm.rr.bsl[[nm]]$Time == 0)
64   chm.rr.bsl[[nm]]$mV <- (chm.rr.bsl[[nm]]$mV / chm.rr.bsl[[nm]]$mV[a]) * 100
65 }
66
67 # Predictor
68 ## Setup data frame
69 chrm <- data.frame(Time = chm.rr.bsl$A1$Time)
70 for(nm in names(chm.rr.bsl)){
71   chrm[nm] <- chm.rr.bsl[[nm]]$mV
72 }
73

```

```

74 ## Input data frame
75 chrM.df <- as.data.frame(t(chrM[, -1]))
76 colnames(chrM.df) <- paste('T', chrM$time, sep = '')
77 chrM.df['Target'] <- as.factor(gsub('\\d', '', colnames(chrM)[-1]))
78 chrM.df['Replicate'] <- gsub('[A-Z]', '', colnames(chrM)[-1])
79
80 ## Data Division
81 ### Training Data
82 chrM.trn <- chrM.df[which(chrM.df$Replicate == 1 | chrM.df$Replicate == 3 | chrM.df$Replicate == 4),]
83 x <- chrM.trn[, -which(colnames(chrM.trn) == "Target" | colnames(chrM.trn) == "Replicate" | colnames(chrM.trn) == 'T0')]
84 y <- chrM.trn[, "Target"]
85
86 ### Validation Data
87 chrM.vld <- chrM.df[which(chrM.df$Replicate == 2),]
88 x.vld <- spct.vld[, -which(colnames(spct.vld) == "Target" | colnames(spct.vld) == "Replicate")]
89 y.vld <- spct.vld[, "Target"]
90
91 ## Predictor Setup
92 ### Model train
93 trnctrl <- trainControl(method = "repeatedcv",
94                         number = 10,
95                         repeats = 5,
96                         verboseIter = T)
97
98 ## Model Training without extra pre-processing
99 ### Random Forests
100 set.seed(123)
101 mdl.raw.rf <- train(x, y,
102                   method = 'rf',
103                   trControl = trnctrl)
104 ### C5.0
105 set.seed(123)
106 mdl.raw.C50 <- train(x, y,
107                    method = 'C5.0',
108                    trControl = trnctrl)
109
110 ## Predictor Evaluation
111 ### Random Forests
112 confusionMatrix(predict(mdl.raw.rf), y)
113 confusionMatrix(predict(mdl.raw.rf, x.vld), y.vld)
114
115 ### C5.0
116 confusionMatrix(predict(mdl.raw.C50), y)
117 confusionMatrix(predict(mdl.raw.C50, x.vld), y.vld)
118
119 ## Model Training with PCA pre-processing
120 ### Random Forests
121 set.seed(123)
122 mdl.pca.rf <- train(x, y,
123                   method = 'rf',
124                   trControl = trnctrl,
125                   preProcess = c('pca'))
126 ### C5.0
127 set.seed(123)
128 mdl.pca.C50 <- train(x, y,
129                    method = 'C5.0',
130                    trControl = trnctrl,
131                    preProcess = c('pca'))
132
133 ## Predictor Evaluation
134 ### Random Forests
135 confusionMatrix(predict(mdl.pca.rf), y)
136 confusionMatrix(predict(mdl.pca.rf, x.vld), y.vld)
137
138 ### C5.0
139 confusionMatrix(predict(mdl.pca.C50), y)
140 confusionMatrix(predict(mdl.pca.C50, x.vld), y.vld)

```

Combined analysis (Spectra and intact chromatograms)

```

1 # Clean environment
2 rm(list=ls())
3 cat("\n14")
4
5 # Load auxiliary functions and libraries
6 source("scripts/functions.R")
7 source("scripts/libraries.R")
8
9 # Data pre-processing
10 ## Load Data
11 ### Run subsequently after R object is saved
12 load(file = 'Data/FTIR.predictor_dfs.RData')
13 load(file = 'Data/Intact.predictor_dfs.RData')
14
15
16 # Predictor
17 ## Setup data frame
18 ammo.ftir <- data.frame(Wavenumber = spectra.n$A1$Wavenumber)
19 for(nm in names(spectra.n)){
20   ammo.ftir[nm] <- spectra.n[[nm]]$Transmittance
21 }
22
23 ammo.ftir.df <- as.data.frame(t(ammo.ftir[, -1]))
24 colnames(ammo.ftir.df) <- paste('T', ammo.ftir$Wavenumber, sep='')
25 ammo.ftir.df['Target'] <- as.factor(gsub('\d', '', colnames(ammo.ftir)[-1]))
26 ammo.ftir.df['Replicate'] <- gsub('[A-Z]', '', colnames(ammo.ftir)[-1])
27
28 ammo.gc <- data.frame(Time = chrn.rr.bsl$A1$Time)
29 for(nm in names(chrn.rr.bsl)){
30   ammo.gc[nm] <- chrn.rr.bsl[[nm]]$mV
31 }
32
33 ammo.gc.df <- as.data.frame(t(ammo.gc[, -1]))
34 colnames(ammo.gc.df) <- paste('T', ammo.gc$Time, sep='')
35 ammo.gc.df['Target'] <- as.factor(gsub('\d', '', colnames(ammo.gc)[-1]))
36 ammo.gc.df['Replicate'] <- gsub('[A-Z]', '', colnames(ammo.gc)[-1])
37
38 ammo <- cbind(ammo.ftir.df, ammo.gc.df)
39
40 ## Data Division
41 ### Training Data
42 ammo.trn <- ammo[which(ammo$Replicate == 1 | ammo$Replicate == 3 | ammo$Replicate == 4),]
43 x <- ammo.trn[, -which(colnames(ammo.trn) == "Target" | colnames(ammo.trn) == "Replicate" | colnames(ammo.trn) == 'T0')]
44 y <- ammo.trn[, "Target"]
45
46 ### Validation Data
47 ammo.vld <- ammo[which(ammo$Replicate == 2),]
48 x.vld <- ammo.vld[, -which(colnames(ammo.vld) == "Target" | colnames(ammo.vld) == "Replicate" | colnames(ammo.vld) == 'T0')]
49 y.vld <- ammo.vld[, "Target"]
50
51 ## Predictor Setup
52 ## Model train
53 trnctrl <- trainControl(method = "repeatedcv",
54                         number = 10,
55                         repeats = 5,
56                         verboseIter = T)
57
58 ## Model Training without extra pre-processing
59 ### Random Forests
60 set.seed(123)
61 mdl.raw.rf <- train(x, y,
62                   method = 'rf',
63                   trControl = trnctrl)
64
65 ### C5.0
66 set.seed(123)
67 mdl.raw.C50 <- train(x, y,
68                    method = 'C5.0',
69                    trControl = trnctrl)
70
71 ## Predictor Evaluation
72 ### Random Forests
73 confusionMatrix(predict(mdl.raw.rf), y)
74 confusionMatrix(predict(mdl.raw.rf, x.vld), y.vld)
75
76 ### C5.0
77 confusionMatrix(predict(mdl.raw.C50), y)
78 confusionMatrix(predict(mdl.raw.C50, x.vld), y.vld)
79
80 ## Model Training with PCA pre-processing
81 ### Random Forests
82 set.seed(123)
83 mdl.pca.rf <- train(x, y,
84                   method = 'rf',
85                   trControl = trnctrl,
86                   preProcess = c('pca'))
87
88 ### C5.0
89 set.seed(123)
90 mdl.pca.C50 <- train(x, y,
91                    method = 'C5.0',
92                    trControl = trnctrl,
93                    preProcess = c('pca'))
94
95 ## Predictor Evaluation
96 ### Random Forests
97 confusionMatrix(predict(mdl.pca.rf), y)
98 confusionMatrix(predict(mdl.pca.rf, x.vld), y.vld)
99
100 ### C5.0
101 confusionMatrix(predict(mdl.pca.C50), y)
102 confusionMatrix(predict(mdl.pca.C50, x.vld), y.vld)

```

Auxiliar Functions

```

##' Read.specter
##'
##' @description
##' Reads a .csv file containing spectra data, with the capability of trimming
##' it, in a given time interval
##'
##' @param file Path to a CSV file on the directory containing integration information.
##' @param trim Vector containing two values - the beginning and end of the
##'           region of the chromatogram to keep.
##'
##' @return A data frame with the specter.
##'
##' @examples
##' read.specter(file = 'data/ftir/A1.CSV')
##' read.specter(file = 'data/ftir/A1.CSV', trim = c(0,1800))
##'
read.specter <- function(file, trim = NULL){
  result <- read.csv(file, sep = ";",
                    dec = ".", skip = 2, header = F, col.names = c("Wavenumber", "Transmittance"))
  if(!is.null(trim))
    result <- result[result[,1] <= trim[1] & result[,1] >= trim[2],]
  return(result)
}

##' Read.spectra
##'
##' @description
##' Read all .csv files containing spectra data, in a folder.
##' It has the capability of trimming them, in a given time interval.
##'
##' @param path Path to a folder containing CSV files of spectra.
##' @param trim Vector containing two values - the beginning and end of the
##'           region of the chromatogram to keep (default = NULL).
##'
##' @return A list of data frames with the spectra.
##'
##' @examples
##' read.spectra('data/ftir')
##' read.spectra('data/ftir', trim = c(0,1800))
##'
read.spectra <- function(path, trim = NULL){
  chrm.nm <- sub('.csv|.CSV', '', list.files(path))
  result = list()
  for(nm in chrm.nm){
    result[[nm]] <- read.specter(sprintf("%s/%s.CSV", path, nm), trim = trim)
  }
  return(result)
}

```

```

##' Read.chromatogram
##'
##' @description
##' Reads a .csv file containing chromatographic data, with the capability of trimming
##' it, in a given time interval
##'
##' @param file Path to a CSV file on the directory.
##' @param trim Vector containing two values - the beginning and end of the
##'           region of the chromatogram to keep (default = NULL).
##'
##' @return A data frame with the chromatogram.
##'
##' @examples
##' read.chromatogram('data/gc/intact/raw/A1.CSV')
##' read.chromatogram('data/gc/intact/raw/A1.CSV', trim = c(10,20))
##'
##' @export
read.chromatogram <- function(file, trim = NULL){
  result <- read.csv(file, sep = "\t", dec = ".", header = F,
                    fileEncoding = "UTF-16", col.names = c('Time', 'mV'))
  if(!is.null(trim))
    result <- result[result[,1] >= trim[1] & result[,1] <= trim[2],]
  return(result)
}

##' Read.chromatograms
##'
##' @description
##' Reads all .csv files containing chromatographic data, in a folder.
##' It has the capability of trimming them, in a given time interval.
##'
##' @param path Path to a folder containing CSV files of chromatograms.
##' @param trim Vector containing two values - the beginning and end of the
##'           region of the chromatogram to keep (default = NULL).
##'
##' @return A list of data frames with the chromatograms.
##'
##' @examples
##' read.chromatograms('data/gc/intact/raw/A1.CSV')
##' read.chromatograms('data/gc/intact/raw/A1.CSV', trim = c(10,20))
##'
##' @export
read.chromatograms <- function(path, trim = NULL){
  chrm.nm <- sub('.csv|.CSV', '', list.files(path))
  result = list()
  for(nm in chrm.nm){
    result[[nm]] <- read.chromatogram(sprintf("%s/%s.CSV", path, nm), trim = trim)
  }
  return(result)
}

```

Chemometric profile of gunpowder

```
## Zero alignment
##
## @description
## Allows the identification of two peaks, one belonging to the reference sample and the other to the sample to align.
## The time corresponding to the first peak (reference) is then divided by the time corresponding to the second peak
##
## @param A Data frame of the sample.
##
## @return Vector of the time of the peak of internal standard.
##
## @examples
## zero.alignment(A = data)
##
zero.alignment <- function(A) {
  plot(A, type = 'l')
  a <- identify(A, n = 1)
  return(A[a,'Time'])
}
```

```
## Stretch alignment
##
## @description
## Allows the identification of two peaks, one belonging to the reference sample and the other to the sample to align.
## The time corresponding to the first peak (reference) is then divided by the time corresponding to the second peak
##
## @param A Data frame of the reference sample.
## @param B Data frame of the sample to be normalize.
##
## @return Vector of the reason between selected points.
##
## @examples
## stretch.alignment(A = data.reference, B = data)
##
stretch.alignment <- function(A, B) {
  plot(A, type = 'l')
  points(B, type = 'l', col = 'red')

  a <- identify(A, n = 1)
  b <- identify(B, n = 1)
  return(A[a,'Time']/B[b,'Time'])
}
```

```
## Resolution Reduction
##
## @description
## Reduces the dimensions of data (e. g. Time in a chromatographic data frame), to simplify data analysis.
## The y value for each new dimension will be the minimum value of y in the readings comprised in the Time window.
##
## @param chromatogram Data frame (or list) data with high resolution (high number of readings per second)
##
## @return Data Frame (or list) with a simplified data.
##
## @examples
## resolution.reduction(chromatogram = data)
##
resolution.reduction <- function(chromatogram) {
  l = 0.005
  Time = seq(0,l2,l)
  mV = c()
  for(t in Time){
    mV <- c(mV, chromatogram$mV[which(abs(chromatogram$Time - t) == min(abs(chromatogram$Time - t)))]})
  }
  return(data.frame(Time = Time, mV = mV))
}
```

```
## Subtract.baseline
##
## @description
## Correct the baseline of chromatograms.
##
## @param degree Degrees of liberty of the polynomial function (default = 10).
## @param choose Choose the degrees (write in console) to the correction of the baseline, with plots (default = T).
## @param data Vector of sequential data.
##
## @return Chromatogram with corrected baseline.
##
## @examples
## subtract.baseline(data = data, degree = 10, choose = T)
##
subtract.baseline <- function(data, degree = 10, choose = T){
  require.package('baseline')
  if(choose){
    accept <- F
    while(!accept){
      plot(bsln <- baseline(matrix(data[,2],nrow = 1), method='modpolyfit', degree = degree))
      response <- readline(sprintf("Accept %d degree (y/new value): ",degree))
      if(response == 'y' || response == ''){
        accept <- T
      } else {
        degree <- as.integer(response)
      }
    }
  } else {
    bsln <- baseline(matrix(data[,2],nrow = 1), method='modpolyfit', degree = degree)
  }
  bsln <- as.vector(bsln@corrected)
  data[,2] <- bsln
  attr(data, 'degree') <- degree
  return(data)
}
```

Appendix

```
##' Subtract.baseline.batch
##'
##' @description
##' Correct the baseline of a batch of chromatograms.
##'
##' @param degree Degrees of liberty of the polynomial function (default = 10).
##' @param choose Choose the degrees (write in console) to the correction of the baseline, with plots (default = T).
##' @param data Vector of sequential data.
##'
##' @return Chromatograms with corrected baseline.
##'
##' @examples
##' subtract.baseline.batch(data = data, degree = 10, choose = T)
##'
subtract.baseline.batch <- function(data, degree = 10, choose = T){
  for(i in 1:length(names(data))){
    nm <- names(data)[i]
    print(nm)
    if(length(degree) == 1)
      data[[nm]] <- subtract.baseline(data[[nm]], degree, choose)
    else
      data[[nm]] <- subtract.baseline(data[[nm]], degree[i], FALSE)
  }
  return(data)
}
```

```
##' Require.package
##'
##' @description
##' Installs and loads necessary packages for R.
##'
##' @param package Name of the package needed
##' @param load Option to load the package (load = T) or just install it (load = F) (default = T)
##'
##' @examples
##' require.package('caret')
##'
require.package <- function(package, load = T){
  if(!require(package, character.only = T, quietly = T)){
    install.packages(package)
    require(package, character.only = T)
  }
}
```

